TITLE:

SPIN

Data Analysis Report

Reference: Final

Date of issue: 19/02/2014

Distributed to:

ESA
SPIN consortium

This work is supported by the European Space Agency

DOCUMENT PROPERTIES

Title	SPIN Data Analysis Report
Reference	SPIN_DAR_Final
Issue	01
Revision	03
Status	Final
Date of issue	19/02/2014
Document type	Deliverable

	FUNCTION	NAME	DATE
LEAD AUTHOR	WP13 manager	Alexei Rozanov (UB)	19.02.2014
CONTRIBUTING AUTHORS	WP12 manager WP12 science team WP13 science team WP15 manager WP16 manager WP17 manager WP18 manager	Doug Degenstein (US) Lena Brinkhoff (UB) Katja Weigel (UB) Michaela Hegglin (HS) Jo Urban (CUT) Simo Tukiainen (FMI) Andreas Jonsson (UT)	19.02.2014
REVIEWED BY	External reviewer	Massato Shiotani	24.12.2013
APPROVED BY	Project leader	Michel Van Roozendael	
ISSUED BY	Project manager	Nathalie Kalb	

DOCUMENT CHANGE RECORD

Issue	Revision	Date	Modified items	Observations
01	02	12.02.2014	Figs. 13 – 15 are merged to two plots (Figs. 13 – 14). Text in Sects. 2.2 and 2.3 is adjusted in accordance. Figure 6 is updated. Overview of points to be shown is added to Sect. 1.2.1. Sect. 1.2.2 is updated.	
01	03	19.02.2014	Sects. 4.1 – 4.4 have been	

			updated	

Table of Contents

Executive summary

This document provides a description of the data set available within the Work Packages (WPs) of the SPIN project. The data sets include the aerosol extinction coefficient profiles from SCIAMACHY and OSIRIS, water vapour profiles from SCIAMACHY, climatologies from the SPARC Data Initiative, products from the GOMOS bright limb algorithm, and temperature climatologies from ACE-FTS, MIPAS, and SMR. Where appropriate the evaluation of the product accuracy and error characterization is provided. For the data products needed to be matured development action plans are presented. The accuracy and error characterization is also done for the matured data sets obtained within WP12 (Maturation of SCIAMACHY and OSIRIS aerosol) and WP13 (Maturation of SCIAMACHY water vapour) at the end of the Phase 1 of the project.

Applicable and reference documents

Boone, C. D., et al. (2005), Retrievals for the atmospheric chemistry experiment Fourier-transform spectrometer, Applied Optics, Vol. 44, No. 33, 7218-7231.

Bourassa, A. E., L. A. Rieger, N. D. Lloyd, and D. A. Degenstein (2011), Odin-OSIRIS stratospheric aerosol data product and SAGE III intercomparison, Atmos. Chem. Phys. Discuss., 11, 25,785-25,811, doi:10.5194/acpd-11-25785-2011.

Bourassa, A. E., C. A. McLinden, A. F. Bathgate, B. J. Elash, and D. A. Degenstein (2012), Precision estimate for Odin-OSIRIS limb scatter retrievals, J. Geophys. Res., 117, D04303, doi:10.1029/2011JD016976.

Deshler, T., M. E. Hervig, D. J. Hofmann, J. M. Rosen, and J. B. Liley (2003), Thirty years of in situ stratospheric aerosol size distribution measurements from Laramie, Wyoming (41_N), using balloon-borne instruments, J. Geophys. Res., 108, 4167, doi:10.1029/2002JD002514.

Ernst, F., C. von Savigny, A. Rozanov, V. Rozanov, K.-U. Eichmann, L. A. Brinkhoff, H. Bovensmann, and J. P. Burrows (2012), Global stratospheric aerosol extinction profile retrievals from SCIAMACHY limb-scatter observations, Atmos. Meas. Tech. Discuss., 5, 5993-6035.

Jones, A., J. Urban , D.P. Murtagh, C. Sanchez, K.A. Walker, N. Livesey, L. Froidevaux, M.L. Santee, Analysis of HCl and ClO time series in the upper stratosphere using satellite data sets, Atmos. Chem. Phys. 11, 5321-5333, doi:10.5194/acp-11-5321-2011, 2011.

Khosravi, M., P. Baron, J. Urban , L. Froidevaux, A. Jonsson, Y. Kasai, K. Kuribayashi, C. Mitsuda, D.P. Murtagh, H. Sagawa, M.L. Santee, T.O. Sato, M. Shiotani, M. Suzuki, T. von Clarmann, K.A. Walker and S. Wang, Diurnal variation of stratospheric HOCl, ClO and HO2 at the equator: comparison of 1-D model calculations with measurements by satellite instruments, Atmospheric Chemistry and Physics, 13 (15), 7587-7606, doi=10.5194/acp-13-7587-2013, August 2013.

Khosravi, M., J. Urban , D.P. Murtagh, and S. Brohede, Climatologies of stratospheric short-lived species from Odin/SMR: Methodology for ClO, in proceedings ESA Living Planet Symposium, 9-13 September 2013, Edinburgh (UK), ESA publication series, 2013 (b).

Lossow, S., J. Urban, P. Eriksson, D. Murtagh, and J. Gumbel (2007), Critical parameters for the retrieval of mesospheric water vapour and temperature from Odin/SMR limb measurements at 557 GHz, Advances in Space Research, 40 (6), pp. 835-845, doi: 10.1016/j.asr.2007.05.026.

Sica, R. J., M. R. M. Izawa, K. A. Walker, C. Boone, S. V. Petelina, P. S. Argall, P. Bernath, G. B. Burns, V. Catoire, R. L. Collins, W. H. Daffer, C. De Clercq, Z. Y. Fan, B. J. Firanski, W. J. R. French, P. Gerard, M. Gerding, J. Granville, J. L. Innis, P. Keckhut, T. Kerzenmacher, A. R. Klekociuk, E. Kyrö, J. C. Lambert, E. J. Llewellyn, G. L. Manney, I. S. McDermid, K. Mizutani, Y. Murayama, C. Piccolo, P. Raspollini, M. Ridolfi, C. Robert, W. Steinbrecht, K. B. Strawbridge, K. Strong, R. Stübi, and B. Thurairajah (2008), Validation of the Atmospheric Chemistry Experiment (ACE) version 2.2 temperature using ground-based and space-borne measurements, Atmos. Chem. Phys., 8, 35-62, doi:10.5194/acp-8-35-2008.

Sofieva, V.F., J. Vira, F. Dalaudier, A. Hauchecorne and the GOMOS team (2009), Validation of GOMOS/Envisat high-resolution temperature profiles (HRTP) using spectral analysis, in New Horizons in Occultation Research, Studies in Atmosphere and Climate, eds. A. Steiner, B. Pirscher, U. Foelsche, and G. Kirchengast, pp. 97-107, doi:10.1007/978-3-642-00321-9_9, Springer-Verlag Berlin Heidelberg.

Stiller, G. P., M. Kiefer, E. Eckert, T. von Clarmann, S. Kellmann, M. García-Comas, B. Funke, T. Leblanc, E. Fetzer, L. Froidevaux, M. Gomez, E. Hall, D. Hurst, A. Jordan, N. Kämpfer, A. Lambert, I. S. McDermid, T. McGee, L. Miloshevich, G.Nedoluha, W. Read, M. Schneider, M. Schwartz, C. Straub, G. Toon, L. W. Twigg, K. Walker, and D. N. Whiteman (2012), Validation of MIPAS

IMK/IAA temperature, water vapor, and ozone profiles with MOHAVE-2009 campaign measurements, Atmos. Meas. Tech., 5, 289-320, doi:10.5194/amt-5-289-2012.

Rodgers, C. D. (2000), Inverse methods for atmospheric sounding: theory and practice, World Scientific.

Russell, P. B., and M. P. McCormick (1989), SAGE II aerosol data validation and initial data use - An introduction and overview, J. Geophys. Res., 94, 8335-8338, doi:10.1029/JD094iD06p08335.

Thomason, L. W., and L. R. Poole (1992), Use of Stratospheric Aerosol Properties as Diagnostics of Antarctic Vortex Processes, J. Geophys. Res., 98, 23,003/23,012, doi:10.1029/93JD02461.

Thomason, L. W., L. R. Poole, and T. Deshler (1997), A global climatology of stratospheric aerosol surface area density deduced from Stratospheric Aerosol and Gas Experiment II measurements: 1984-1994, J. Geophys. Res., 102, 8967-8976, doi:10.1029/96JD02962.

Thomason, L. W., and G. Taha (2003), SAGE III aerosol extinction measurements: Initial results, Geophys. Res. Lett., 30, 1631, doi:10.1029/2003GL017317.

von Clarmann, T., N. Glatthor, U. Grabowski, M. Höpfner, S. Kellmann, M. Kiefer, A. Linden, G. M. Tsidu, M. Milz, T. Steck, G. P. Stiller, D. Y. Wang, H. Fischer, B. Funke, S. Gil-López and M. López-Puertas. (2003), Retrieval of temperature and tangent altitude pointing from limb emission spectra recorded from space by the Michelson Interferometer for Passive Atmospheric Sounding (MIPAS), J. Geophys. Res., 108, 4736, doi:10.1029/2003JD003602, D23.

von Clarmann, T., M. Höpfner, S. Kellmann, A. Linden, S. Chauhan, B. Funke, U. Grabowski, N. Glatthor, M. Kiefer, T. Schieferdecker, G. P. Stiller, and S. Versick (2009), Retrieval of temperature, H2O, O3, HNO3, CH4, N2O, ClONO2 and ClO from MIPAS reduced resolution nominal mode limb emission measurements, Atmos. Meas. Tech., 2, 159-175, doi:10.5194/amt-2-159-2009.

Wang, D. Y., T. von Clarmann, H. Fischer, B. Funke, S. Gil-López, N. Glatthor, U. Grabowski, M. Höpfner, M. Kaufmann, S. Kellmann, M. Kiefer, M. E. Koukouli, A. Linden, M. López-Puertas, G. Mengistu Tsidu, M. Milz, T. Steck, G. P. Stiller, A. J. Simmons, A. Dethof, R. Swinbank, C. Marquardt, J. H. Jiang, L. J. Romans, J. Wickert, T. Schmidt, J. Russell III and E. Remsberg (2005), Validation of stratospheric temperatures measured by Michelson Interferometer for Passive Atmospheric Sounding (MIPAS) on Envisat, J. Geophys. Res., 110, D08301, doi:10.1029/2004JD005342.

Wolff, M.A., T. Kerzenmacher, K. Strong, K.A. Walker, M. Toohey, E. Dupuy, P.F. Bernath, C.D. Boone, S. Brohede, V. Catoire, T. von Clarmann, M. Coffey, W.H. Daffer, M. De Mazière, P. Duchatelet, N. Glatthor, D.W.T.Griffith, J. Hannigan, F. Hase, M. Höpfner, M., N. Huret, N. Jones, K. Jucks, A. Kagawa, Y. Kasai, I. Kramer, H. Küllmann, J. Kuttippurath, E. Mahieu, G. Manney, C.T. McElroy, C. McLinden, Y. Mébarki, S. Mikuteit, D. Murtagh, C. Piccolo, P. Raspollini, M. Ridolfi, R. Ruhnke, M. Santee, C. Senten, D. Smale, C. T´etard, J. Urban , and S. Wood, Validation of HNO3 , ClONO2 , and N2 O5 from the Atmospheric Chemistry Experiment Fourier Transform Spectrometer (ACE-FTS), Atmos. Chem. Phys., 8, 3529-3562, 2008.

Wurl, D., R. G. Grainger, A. J. McDonald, and T. Deshler (2010), Optimal estimation retrieval of aerosol microphysical properties from SAGE~II satellite observations in the volcanically unperturbed lower stratosphere, Atmos. Chem. Phys., 10, 4295-4317.

Yue, G. K., C.-H. Lu, and P.-H. Wang (2005), Comparing aerosol extinctions measured by Stratospheric Aerosol and Gas Experiment (SAGE) II and III satellite experiments in 2002 and 2003, J. Geophys. Res., 110, D11,202, doi:10.1029/2004JD005421.

Acronyms and abbreviations

ACE-FTS - Atmospheric Chemistry Experiment - Fourier Transform Spectrometer
AVK - Averaging Kernel
CHAMP - CHAllenging Mini-satellite Payload
ECMWF - European Centre for Medium-Range Weather Forecasts
ENVISAT - Environmental Satellite
ESA - European Space Agency
GBL - GOMOS bright limb
GOMOS - Global Ozone Monitoring by Occultation of Stars
GRACE - Gravity Recovery and Climate Experiment
HALOE - The Halogen Occultation Experiment
MIPAS - Michelson Interferometer for Passive Atmospheric Sounding
MLS - Microwave Limb Sounder
MPV - modified potential vorticity
NCEP - National Centers for Environmental Prediction
OSIRIS - Optical System for Imaging and low Resolution Integrated Spectroscopy
POAM - Polar Ozone and Aerosol Measurement
PVU - Potential Vorticity Units
RO - Radio Occultation
SAD - Surface Area Density
SAGE - Stratospheric Aerosol and Gas Experiment
SAR - Synthetic Aperture Radar
SCIAMACHY - Scanning Imaging Absorption Spectrometer for Atmospheric ChartographY
SCODA - SCIAMACHY Cloud Detection Algorithm
SMILES - Superconducting Submillimeter-Wave Limb-Emission Sounder
SMR - Sub-Millimetre Radiometer
SPARC - Stratosphere-troposphere Processes And their Role in Climate
SPIN - ESA SPARC Initiative
WP - Work Package
TSX - TerraSAR-X

Introduction

This document provides details on several data sets which were either delivered by the respective science teams at the beginning of the project or were generated within Phase 1 of the project. The first group of products includes the aerosol extinction coefficient data sets from OSIRIS and SCIAMACHY (WP12), the water vapour profile data set from SCIAMACHY (WP13) and the climatologies generated within the SPARC Data Initiative (WP15). As these data sets (with exception of the SPARC Data Initiative climatologies) have been matured within Phase 1 of SPIN, an assessment of the accuracy of the original data sets and characterization of errors needed to be performed already in the early stages of the project. The results of this assessment presented in this document were then used to inform the maturation strategy. The latter is outlined below in the form of the action plans to develop the matured products.
For the SPARC Data Initiative climatologies (WP15), the assessment of the level-3 data quality represents the main deliverable of the work package which is being published in the SPARC Data Initiative report and in journal publications. A quality assessment of the level-2 data that were used to produce the level-3 climatologies is provided in this document.
At the end of Phase 1 of the project an assessment of the quality of the data sets produced within SPIN such as improved short-lived species climatologies (WP16), GOMOS bright limb (WP17), and temperature climatologies (WP18) was performed. Furthermore, an assessment of the accuracy of the matured OSIRIS and SCIAMACHY products generated within WP12 and WP13 was performed. The assessments results are also presented in this document.

1. WP 12: Maturation of SCIAMACHY and OSIRIS aerosol

1.1. Status of the products

1.1.1. OSIRIS

The OSIRIS instrument was launched in February 2001 on board the Odin satellite and continues full operation. Odin was placed into a polar, sun-synchronous orbit with an inclination of 98º from the equator. Since OSIRIS views in the orbital plane this provides measurements from 82°S to 82°N with equatorial crossings at 1800 h and 0600 h for the north and southbound crossings, respectively. This dusk/dawn orbit provides coverage of a large latitude range, but also restricts OSIRIS from taking measurements in the winter hemisphere, as this portion of the globe is not sunlit. Prior to 2007 OSIRIS spent approximately every second day in aeronomy mode during which time approximately 500 sunlit profiles per day were taken. After 2007 OSIRIS switch to fulltime aeronomy mode.

Vertical profiles of the Version 5.07 aerosol extinction coefficient have been processed from November 2001 to the present and are publicly available at: http://odin-osiris.usask.ca/?q=node/280. Work on a matured aerosol extinction product (Version 6.00) has been underway, and processing of the full mission is now complete. This version incorporates the 1.53µm infrared channel to retrieve a particle size parameter with the extinction coefficient.

1.1.2. SCIAMACHY

SCIAMACHY was launched in March 2002 onboard the European satellite Envisat and ceased its operation in April 2012 with a loss of Envisat. SCIAMACHY was in a sun-synchronous orbit with an inclination of 98.55^{o} and a 10 a.m. equator crossing time. As the limb-scatter measurements used to retrieve the vertical profiles of the aerosol extinction coefficient are restricted to the sunlight conditions, the latutde coverage of SCIAMACHY data varies from about 85 deg in the summer hemisphere to about 60 deg in the winter hemisphere.
Vertical profiles of the aerosol extinction coefficient from SCIAMACHY (V1.0) are available from August 2002 up to April 2012 (loss of ENVISAT) at http://www.iup.physik.uni-bremen.de/scia-arc. The retrieval is based on SCIAMACHY Level 1 data version 7.03. The Level 1 data were calibrated with all calibration options but flags 0, 6, and 7, i.e., memory effect correction, polarization correction and absolute calibration were not performed due to remaining issues with these calibration steps.

1.2. Product accuracy and error characterization

1.2.1. OSIRIS

The accuracy of the Version 5.07 aerosol data product was discussed by *Bourassa et al.* (2011) through comparison of coincident SAGE III measurements. Typical biases were less than 10% at altitudes near the peak of the Junge layer. The random error associated with the aerosol data product is estimated to be between 12-17 percent over from 20 to 30 kilometres increasing up to 30 percent at 35 km. The precision has been verified using matched pairs and the Fioletov method (Bourassa, 2012), but it is reasonable to say this verification is not a complete validation of the method used to calculate the random error. The primary issue with Version 5.07 of the OSIRIS aerosol product is the requirement that the particle size distribution be assumed before extinction can be retrieved. Currently, the particle size distribution is assumed to be a lognormal with a mode radius of 0.08μm and mode width of 1.6. Error in these assumed quantities produces an incorrect phase function in the forward model and error in the retrieved extinction parameter. Version 6.00 of the aerosol retrieval seeks to improve this by retrieving the extinction and the mode radius parameter of the lognormal distribution. The Version 6.00 results in this report include:

- Substantially improved biases between coincident ascending and descending node measuremrents in the tropics. Mid-to-high latitudes showed much less systematic bias in Version 5.07, and therefore little improvement in Version 6.00.
- Coincident comparisons to SAGE III show typical differences of 10-15% in 750 nm extinction, although this includes only mid-to-high latitude measurements between 2002 and 2005.
- Angstrom coefficient retrievals show good qualitative agreement with SAGE II in the tropics, although due to the wavelength differences of the instruments a more quantative analysis was not performed at this time.
- The Version 6.00 retrievals do not retrieve albedo at 1.53 μm and this is likely causing a systematic error in the retrievals. The error is both time and latitude dependent and typically ranges from 5-30% error in extinction depending on solar geometry.
- Precision analysis shows the error in extinction due to measurerment noise to be approximately 10-15% at the peak of the aerosol layer, although this will vary depending on measurement geometry.

1.2.2. SCIAMACHY

A detailed description of the accuracy and error characterization for SCIAMACHY aerosol retrieval V1.0 is given by (Ernst et. al., 2012) and briefly summazized below.

- The investigations showed that the retrieved stratospheric aerosol extinction profiles of the limb-scatter SCIAMACHY data set (from 2003–11) shows good qualitative results on the aerosol variation during almost a whole decade: Volcanic eruptions and bushfires can clearly be identified and a seasonal cycle with a maximum of the extinction coefficient in winter becomes apparent as well as a pronounced biannual variation in higher altitudes. Furthermore, the observed aerosol variations are consistent with lidar measurements
- Comparisons with co-located SAGE II sun occultation measurements from 2002 - 2005 resulted in a globally averaged difference of less than 20% between 15 and 35 km altitude and less than 10% between 16 and 30 km.
- Comparisons made for 20° latitude bins showed the presence of systematic interhemispheric differences, with SCIAMACHY overestimating aerosol extinction in the southern hemisphere and underestimating in the northern hemisphere at mid- and high latitudes.
- The largest difference compared to SAGE II is about +50% at an altitude of 20 km at 40-60°S and -50% between 25 and 30 km at 60-80°N

For the matured SCIAMACHY aerosol retrieval V1.1 comparisons with SAGE II measurements have been redone showing a much better agreement in most of altitude and latitude ranges. A deailed description of the results is given in Sect. 1.4.2.

1.3. Action plans to develop matured products

1.3.1. OSIRIS

In order to mature this data product, the OSIRIS team has developed and tested algorithms to determine parameters of the particle size distribution from the measurements themselves. Inclusion of the 1.53 micron radiance measurements made by the OSIRIS infrared imager channels has shown much promise for the determination of one mode of the distribution. Due to the inclusion of the infrared data however, this product is considerably noisier than Version 5.07. In addition, the Infrared detector can saturate when measuring high levels of aerosol, biasing results. To improve this, while still limiting the effect of particle size on the extinction retrieval, a mode radius climatology will be developed to help reduce the noise of individual measurements. This particle size climatology will then be used with an algorithm similar to Version 5.07 to develop an improved aerosol extinction coefficient, which minimizes the problems due to incorrect particle size as well as those associated with the using the noisier infrared channel. An example of a climatological map is shown in Figure 1. Here, the retrieved Angstrom coefficient has been averaged over distance, time and altitude to produce an Angstrom coefficient map for February 26th, 2004 at 25km altitude. The averaging used here greatly reduces noise associated with individual measurements and produces a climatology usable with the 750nm measurements.

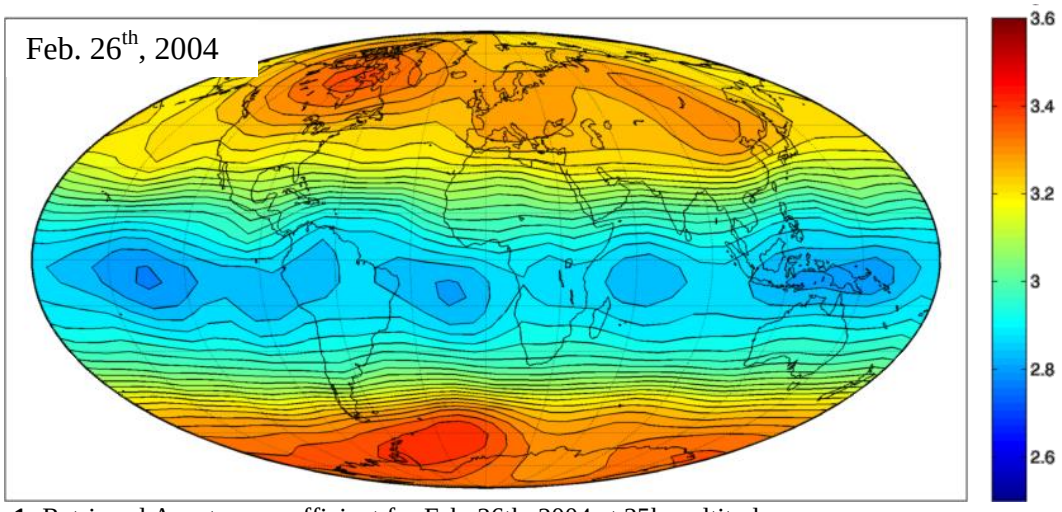

Figure 1: Retrieved Angstrom coefficient for Feb. 26th, 2004 at 25km altitude.

1.3.2. SCIAMACHY

The overall goal is to improve the accuracy of the existing SCIAMACHY aerosol data set from 2002 to 2012 and provide reliable quantitative information for climatological interpretation.

- To reduce the error in the aerosol extinction profiles in general and the interhemispheric difference in particular, the focus will be on the phase function. The latter is most likely responsible for the difference because of the change of the single scattering angle with the latitude associated with the SCIAMACHY limb viewing geometry.
- Some potential error sources for this phenomenon, like sensitivity to errors in the assumed ground albedo, have already been excluded.
- An examination of the synthetic retrievals to simulate different volcanic scenarios for different latitude regions is planned.
- The synthetic retrieval of a strong volcanic aerosol load has to be investigated.
- It is intended to be checked whether a measurement vector based on a single wavelength provides a more accurate retrieval result than the currently used color index approach.

1.4. Characterisation of the matured products

1.4.1. OSIRIS

Estimation of the accuracy and precision of the OSIRIS Version 6.00 aerosol retrieval is estimated through comparison with the SAGE II and SAGE III satellites as well an error analysis as outlined by *Rodgers* (2000).

In operation from 2001 until 2005, SAGE III measured aerosol extinction profiles at nine wavelengths, ranging from 385 to 1545nm (*Thomason*, 2003). SAGE III was launched into a polar orbit, performing occultations in the mid to polar latitudes. With an accuracy and precision on the order of 10%, and a channel at 755nm, SAGE III provides an excellent data set for comparison (*Thomason*, 2010). *Bourassa et al*. (2011) compared the Version 5.07 algorithm with coincident SAGE III measurements using a coincident criteria of ±6 hours, ±1° latitude and ±2.5° longitude. These criteria provide 479 coincident measurements, of which 359 have successful Version 6.00 retrievals.

The average percent difference between the SAGE III and Version 6.00 OSIRIS measurements are shown in : **Percent difference between SAGE III and OSIRSIS coincident measurements**. The left panel shows the difference in 750nm extinction with 1530nm difference shown on the right. Typically, 750nm OSIRIS measurements are within 10% of the 755nm SAGE III measurements, although above 25km OSIRIS underestimate by up to 20%. Comparison of the 1530nm OSIRIS extinction and 1545nm SAGE III extinction is somewhat less favourable, with OSIRIS measuring approximately 15% smaller extinction values below 23km and 40% smaller values above 25km.

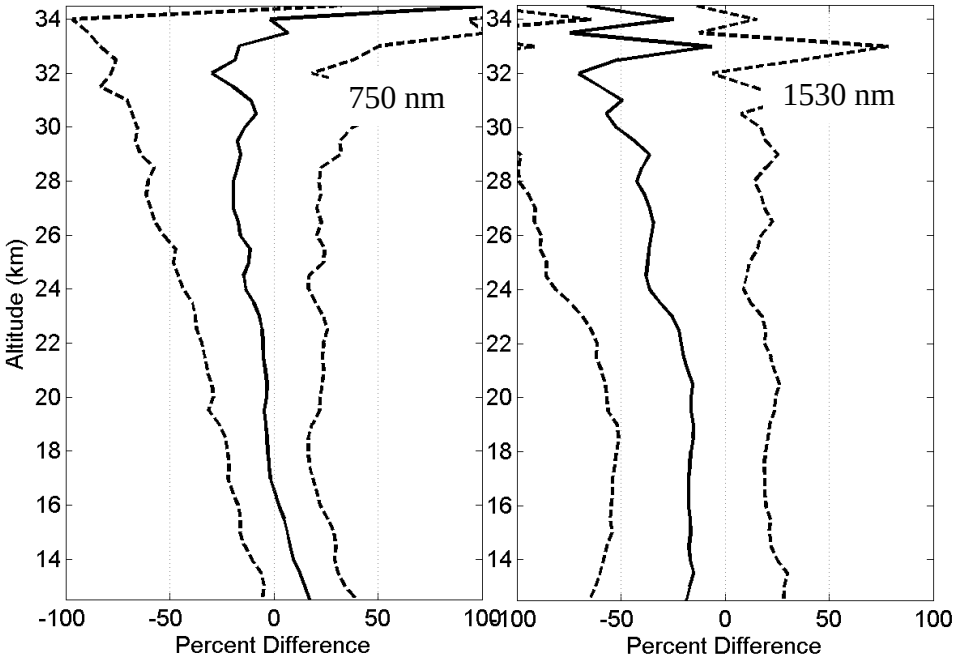

Figure 2: Percent difference between SAGE III and OSIRSIS coincident measurements at similar wavelengths. Solid lines are the percent difference with one standard deviation shown as dashed. The difference between OSIRIS 750nm and SAGE III 755nm extinction is shown on the left. OSIRIS 1530nm and SAGE III 1545nm channels are on the right.

SAGE II (*Russell*, 1989) was launched in 1985, and continued operating until mid 2005, providing approximately three years of overlap with the OSIRIS mission. SAGE II produced high quality measurements for the duration of its lifetime with the 525 and 1020nm channels agreeing well with SAGE III, with typical uncertainties less than 15% for the majority of the aerosol layer (*Yue*, 2005). This overlap period also contains good tropical coverage with two volcanic eruptions: Mts. Ruang (Ru) and Reventador (Ra) in 2003, and Mt. Manam (Ma) in 2005, providing a good test of the OSIRIS particle size retrieval. Although SAGE II has no 750nm channel the angstrom coefficient as measured by SAGE II between 525 and 1020nm can be used to convert the 525 and 1020nm extinction measurements to a comparable wavelength. Figure 3 shows the monthly 750nm extinction ratio as measured by OSIRIS (top panel) and SAGE II V7.00A (bottom panel) between 20N and 20S. Agreement is generally excellent with typical differences of 10-20%. Although OSIRIS underestimates low altitude volcanic conditions this is due to the infrared channel which tends to saturate in these conditions causing a measurement bias to low aerosol conditions. This is addressed in section 2.3.1 of the OSIRIS action plan.

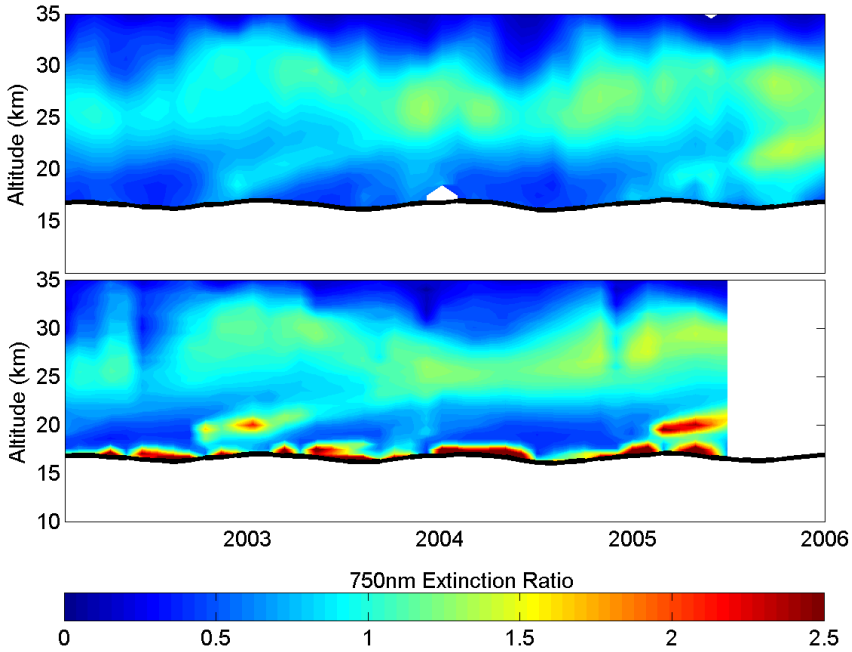

Figure 3: Monthly averaged 750nm extinction ratio in the tropics. OSIRIS measurements shown in the top panel with SAGE II V7.00A in the bottom panel.

Assuming a linear relationship between extinction and wavelength (in logarithmic space) allows one to compute the Angstrom coefficient from the relationship (*Angstrom*, 1964):

$$\frac{\sigma_{\mathrm{aer}}(\lambda_1)}{\sigma_{\mathrm{aer}}(\lambda_0)} = \left(\frac{\lambda_1}{\lambda_0}\right)^{-\alpha}.$$

This relationship is only approximate however, and Angstrom coefficients determined from extinction coefficients at different wavelengths are not expected to be identical. Although the SAGE II angstrom coefficient is not directly comparable to the Angstrom value retrieved by OSIRIS due to the wavelength difference, large scale features such as altitude dependence and volcanic eruptions are visible in both datasets. Figure 4 shows the monthly averaged OSIRIS and SAGE II Angstrom coefficients (V7.00A) from 20N to 20S. Aerosol particles decrease in size with altitude and after the smaller volcanic eruptions of Ruang/Raventador and Mt. Manam. A two year cycle is also present that correlates well with the QBO. Although general qualitative agreement is good OSIRIS also measures a 6 month cycle. This may be due to the change in solar zenith angle with the Odin orbit, which when coupled with the error in the 1.53µm albedo, presents as a particle size error with a biannual cycle.

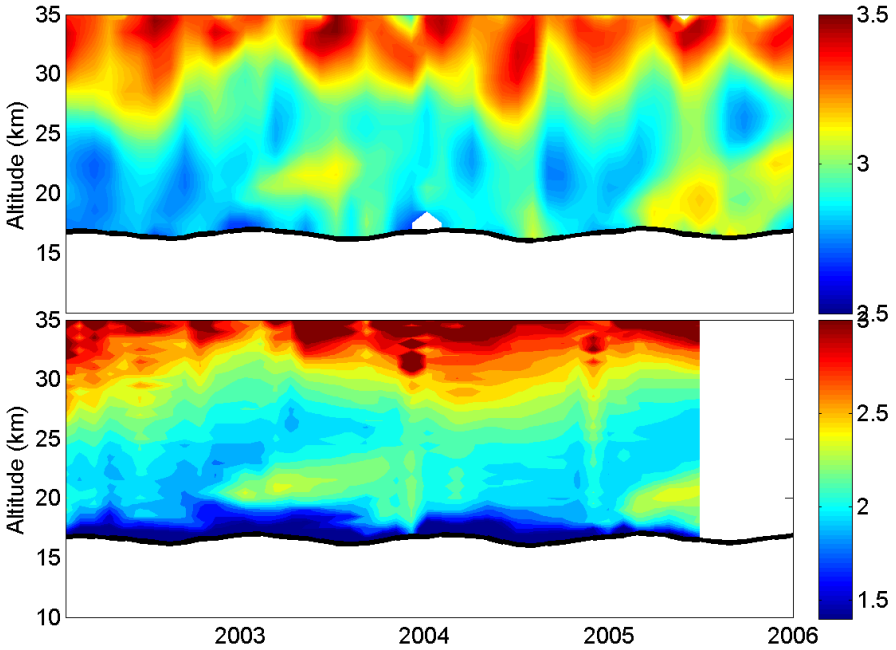

Figure 4: Top panel is the monthly OSIRIS Angstrom coefficient from 750 to 1530nm from 20N to 20S. Bottom panel is the same picture with the SAGE II Angstrom coefficient (V7.00A) from 525 to 1020nm. Angstrom coefficient is given by the color scale to the right of the respective panels.

Although the SAGE II Angstrom component is not directly comparable to OSIRIS retrievals the surface area density (SAD) has also been derived from SAGE II extinction measurements (Thomason, 1992, 1997). The SAD can also be found from OSIRIS measurements through the retrieved lognormal distribution and extinction. Figure 5 shows the monthly averaged OSIRIS and SAGE II SAD retrievals (V7.00A) for 20N to 20S. Generally, agreement is good; however, OSIRIS measures slightly larger SAD values in the volcanic plumes and slightly lower values at high altitudes. This may be partially explained by the insensitivity of the SAGE II inversion to particles smaller than 100nm (*Wurl*, 2010; *Deshler*, 2003).

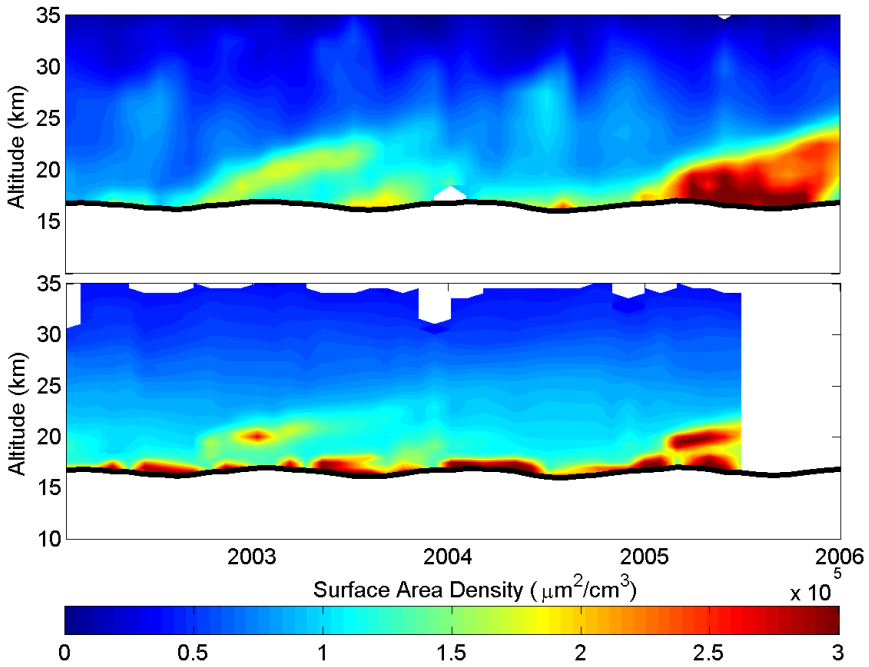

Figure 5: Monthly averaged surface area density from OSIRIS in the top panel and SAGE II (V7.00A) in the bottom panel.

The error in assumed particle size was evident in the Version 5 aerosol product through the comparison of measurements taken with similar atmospheric conditions but with different viewing geometries. Because the phase function was incorrect, the retrieval was dependent on the solar scattering angle. This is visible in the daily averaged extinction ratio between 20 and 32km in the tropics when the measurements are split into the ascending and descending tracks, as shown in Figure 6. Here a systematic difference between the measurements is evident, as well as a high correlation with the scattering angle. The Version 6 product, shown in the right column of Figure 6, has much smaller discrepencies between measurements of different scattering angles. The yearly cycle in the measured extinction is still present, particulary after 2006 when volcanic activity is higher; however it is now measured by both the ascending and descending tracks independently. As well, a yearly cycle in the stratospheric aerosol is not unexpected as it has been measured by LIDARs in Mauna Loa and Boulder Colorado (Hoffman, 2010) as well as in Japan (Uchino, 2012).

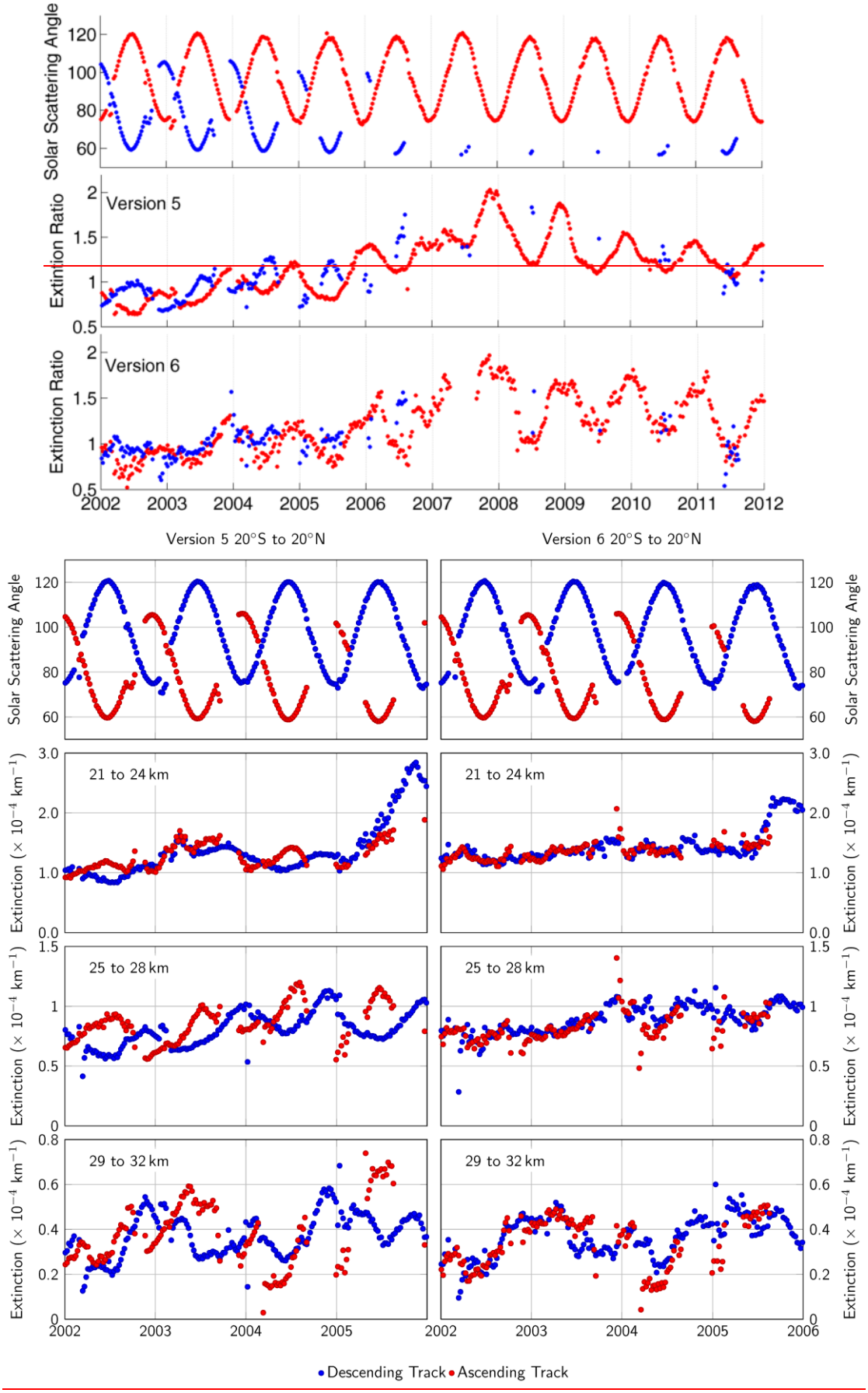
Solar Scattering Angle
Extinction Ratio
Version 5
Extinction Ratio
Version 6
2002
2003
2004
2005
2006
2007
2008
2009
2010
2011
2012
Version 5 20°S to 20°N
Version 6 20°S to 20°N
Solar Scattering Angle
Extinction (× 10⁻⁴ km⁻¹)
21 to 24 km
25 to 28 km
29 to 32 km
Descending Track
Ascending Track

Figure 6: Comparison of weekly averaged 750 nm extinction retrieved using Version 5.07 (left column) and Version 6.00 (right column) at three altitude levels. The top row shows the solar scattering angles of the ascending and descending nodes.

The measurement error for the optical spectrograph and infrared imager is quite different due to the measurement techniques. As the optical spectrograph is scanned vertically the exposure time is changed, resulting in approximately the same number of photons being counted with each exposure; resulting in noise that increases only slightly with altitude, ranging from approximately 0.5-1% of the total signal. The IR channels image the entire vertical profile simultaneously, resulting in considerable noise at higher altitudes, typically on the order of 10%. Fortunately, the imager takes multiple profiles for each optical spectrograph scan, often 30 or more, which can be collapsed into an average profile to reduce the noise. Despite this averaging, error in the infrared channel still exceeds that of the optical spectrograph. This produces a measurement vector error of approximately 5% in infrared and 1% at 750nm. In the retrieved quantities this translates to an error of 10% near the peak of the aerosol layer.

The averaging kernel matrices for the extinction and mode radius quantities are shown in Figure 7. These are calculated numerically by perturbation of a typical aerosol extinction and mode radius profile at each altitude and successive retrieval using simulated radiances for each state. The averaging kernel for extinction is very nearly unity for 10km and above, with very little smoothing of the profile, as was seen in the Version 5 algorithm. The resulting smoothing error in extinction is typically less than 5% for most altitudes, although this increases to more than 10% below 10km. Changes in mode radius are not captured as accurately at altitudes below 15km with approximately half of the change being added to the perturbed altitude. Despite the larger off diagonal elements in the mode radius averaging kernel, error for typical cases is limited to less than 10% due to more accurate a priori estimates.

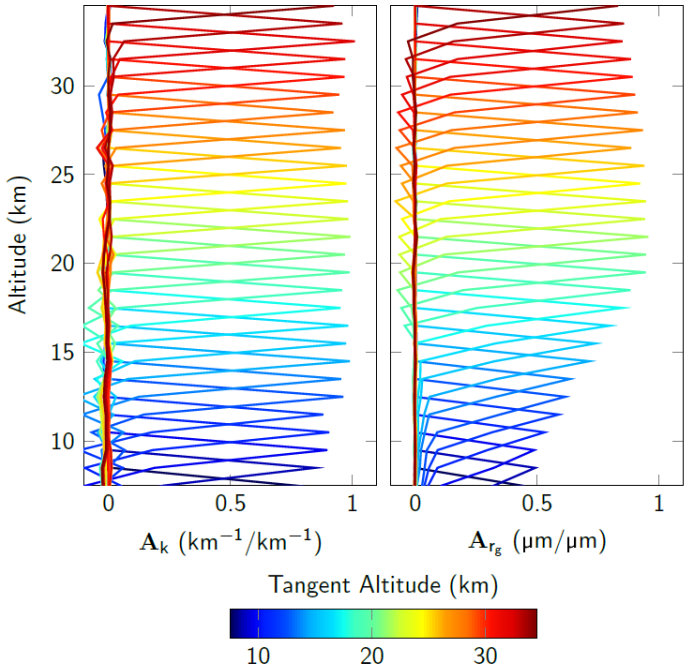

Figure 7: The extinction (left) and mode radius (right) averaging kernels.

One of the largest uncertainties results from the unknown albedo at 1.53µm. Although the albedo is retrieved at 750nm, the same cannot currently be done at 1.53µm due to a lack of an absolute calibration in the infrared channels. The immediate solution is to assume the 1.53µm albedo is unchanged from that at 750nm. Simulated retrievals show that if the error in the 1.53µm albedo is 0.5, this causes an error of approximately 5-30% in the retrieved quantities depending on solar zenith and scattering angles.

A scan with a forward geometry was simulated and the relative errors due to measurement, smoothing and 1.53µm albedo are shown in Figure 8. At altitudes above 30km and below 15km error begins to dominate the signal, with virtually all of the error due to measurement noise. In the bulk of the aerosol layer this error reduces to approximately 10% for both retrieved quantities. The error budget is primarily due to the 1.53µm measurements, which are approximately 5-10 times noisier than the 750nm measurements.

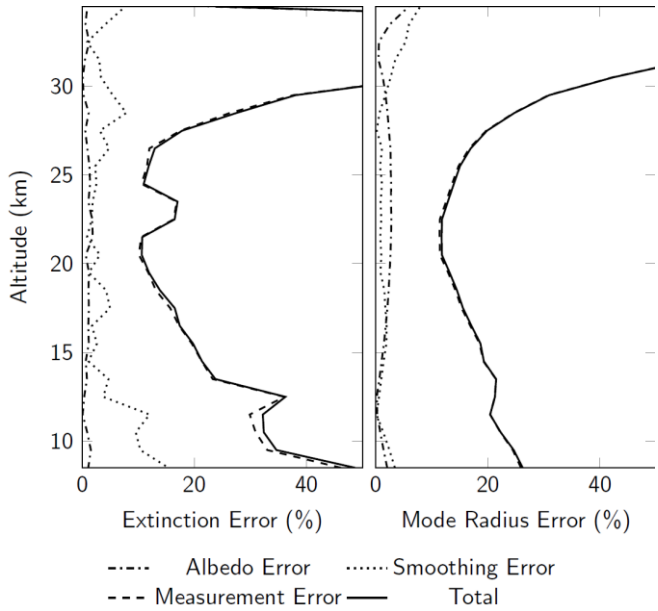

Figure 8: Total percent error in retrieved extinction and mode radius due to albedo, smoothing and measurement error.

Although mode radius is the particle size parameter adjusted in the model, it is sensitive to the true mode width and the presence of a second mode of larger particles. This is mitigated by converting the mode radius to the Angstrom coefficient. The efficacy of this conversion was tested by simulating OSIRIS measurements when the true state was largely bimodal where the fine mode has a width of 1.75 and mode radius of 90nm. A second, course mode of particles was also added with a mode width of 1.2 and mode radius of 400nm. The peak 750nm aerosol extinction was set to be $7 \cdot 10^{-4} km^{-1}$ with approximately half of this coming from the course mode at 22km. As altitude increases the course mode fraction decreases to simulate a more realistic profile. The retrieved aerosol was assumed to have a single mode of particles with a mode width of 1.6. Simulated retrievals were performed for 765 OSIRIS measurements with a variety of scattering and zenith angles. The mean error and standard deviation of the retrieved extinction and Angstrom coefficient are shown in Figure 9. Error in the retrieved extinction was typically 5-10% with an error in the Angstrom coefficient of 10-15%. This shows that even under largely bimodal conditions the coupled retrieval of extinction and mode radius produce robust results with little bias and a small dependence on measurement geometry.

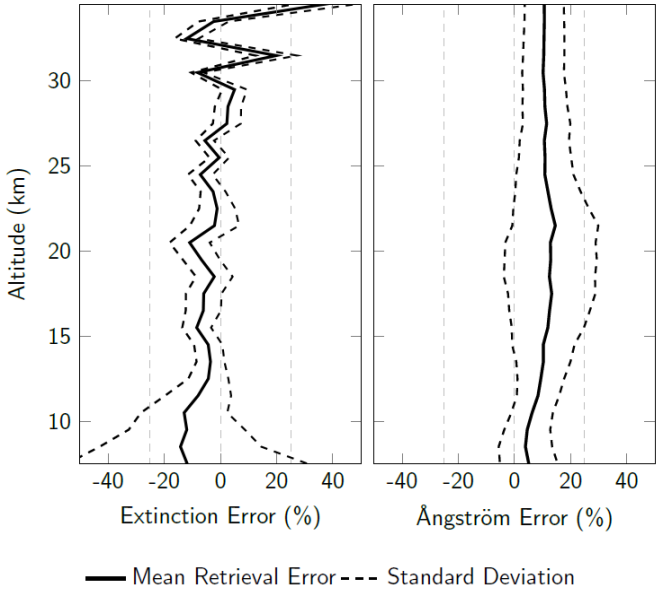

Figure 9: Error in retrieved extinction and Angstrom coefficient due to error in particle size assumptions.

1.4.2. SCIAMACHY

The accuracy of the SCIAMACHY aerosol extinction coefficients V1.1 is estimated comparing SCIAMACHY aerosol profiles at 525 nm with co-located SAGE II data (V6.2). The comparison results for 8 latitude bins are presented in Figure 10. At middle and high southern latitudes (40°-80°S) the results are much closer to the SAGE II extinctions as compared to the previous retrieval version. Between 15 and 27 km altitude, the difference to SAGE II is now between - 10 and - 20% compared to + 30 to + 60% in Version 1.0. At the same latitudes of the northern hemisphere the quality of the retrieval remains more or less the same. Between 60°N and 80°N the difference to SAGE II is slightly smaller in the 15-23 km altitude range (- 15 to + 10%), while it increases up to -50% above. Between 40° and 60°N there is almost no difference to the previous retrieval version, which is most probably because the corresponding phase functions are very similar at scattering angles typical for this latitude bin. At all latitude bins between 40°N and 40°S, one observes a shift of the relative difference towards negative values. While for both 20°-40° bins, it is difficult to conclude if the results are better or worse than those from version 1.0, they are definitely worse for latitudes around the equator (20°N-20°S). Here, relative differences of around - 30% are obtained in both bins above the tropopause compared to about + 20% (0°-20°S) and around 0 (0°-20°N) for Version 1.0. Beside the phase function approximation, further sources of potential systematic errors, like the effect of the a priori profiles, errors in the assumed surface albedo, neutral density profiles, ozone profiles, and errors in the tangent height registration, have been analyzed by performing forward model runs with different settings – i.e., introducing artificial errors – for the specific parameter to be investigated, leaving all other settings unchanged.
It turned out that the relative error due to the a priori profile is generally on the order of a few percent and is below 10% even in the worst case. Six modifications of the synthetic retrievals were tested (multiplication with a factor of 0.5 and 2, a height shift of the complete profile by ± 3 kilometers, and an artificial minimum/maximum around an altitude of 25 kilometers).
Furthermore, there is a relative error in the retrieved aerosol extinction coefficient regarding the assumed surface albedo, which is up to 40% in the tropics and about 2% in northern polar regions (changing the albedo from 0 to 1 with respect to 0.5 for five selected latitudes: 83°N, 40°N, 0, 40°S and 75°S). Comparing the two hemispheres – 40°N and 40°S in particular –

indicates that the retrieval is far more sensitive to the ground albedo in the southern hemisphere.

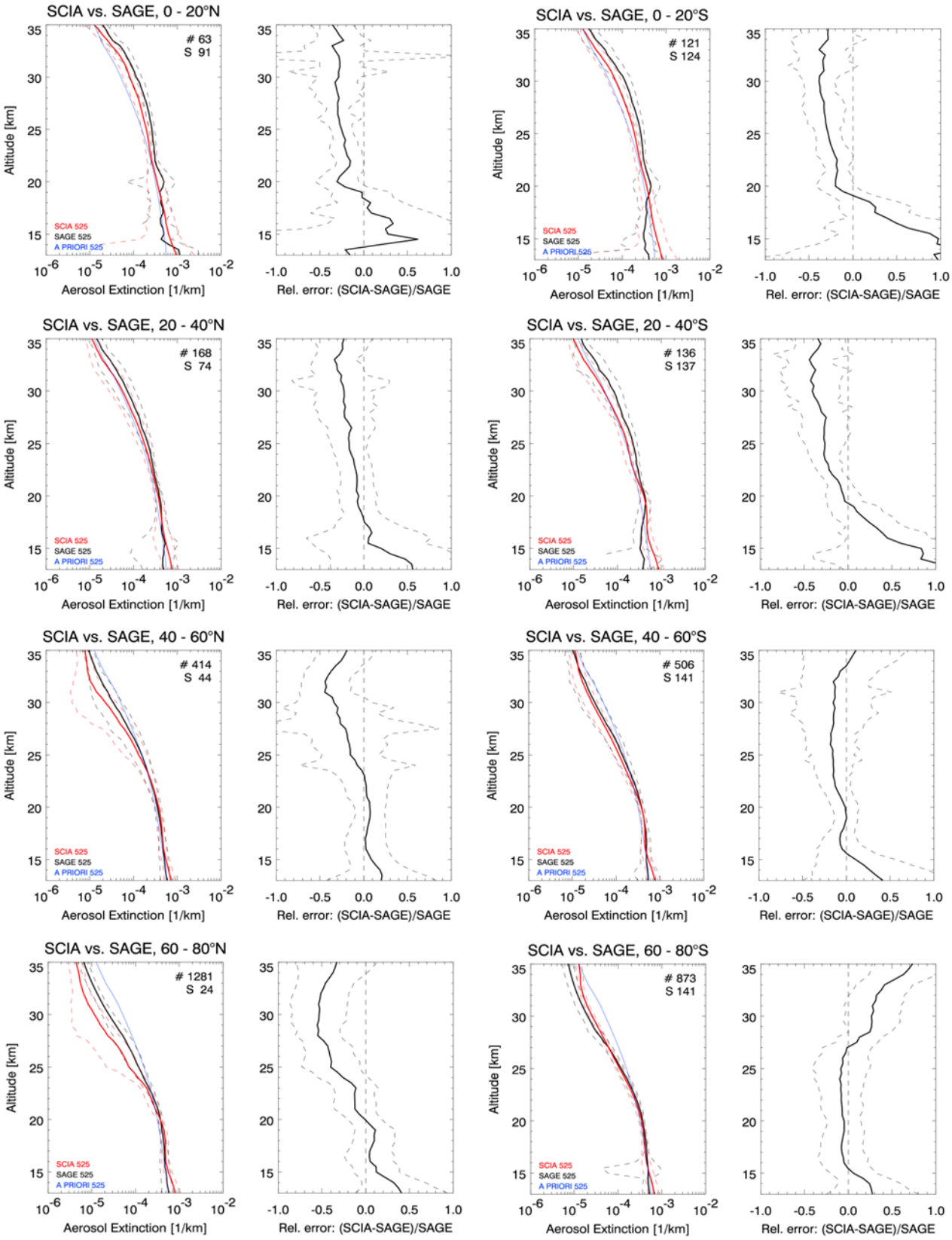

Figure 10: Comparison of the stratospheric aerosol extinction coefficients retrieved from SCIAMACHY limb measurement with co-located data from SAGE II for 8 latitude bins. Left panels: Aerosol extinction coefficient profiles at 525 nm from SCIAMACHY (red) and SAGE II (black) and the a priori profile used for SCIAMACHY retrievals (blue). Dashed lines depict corresponding standard deviations. Right panels: mean relative differences between SCIAMACHY and SAGE II V6.2 results (solid) and corresponding standard deviations (dashed).

2. WP 13: Maturation of SCIAMACHY water vapour

2.1. Status of the products

Water vapour profiles from SCIAMACHY limb measurements V3.0 are available from August 2002 up to April 2012. The dataset covers the altitude range between 11 and 25 km. The precursor version (V2) data set was found to agree to balloon borne measurements within about 20% (Rozanov et al. 2010). Due to an improvement of the calibration settings and a variable aerosol correction an agreement of about 10% with balloon borne measurements could be reached in V3 (Rozanov et al. 2011). The retrieval follows the optimal estimation maximum a posteriori method (Rodger, 2000) using a Gauss-Newton iterative approach. The tangent heights between 11 and 25 km are used. At each tangent height the spectrum is divided by the solar spectrum measures in the same orbit. Only the differential absorption structures are evaluated to reduce the influence of aerosols and surface albedo. Logarithms of the measures radiation and of trace gas number densities are used. In addition to water vapour, methane is included to the retrieval as well as a tropospheric contribution parameter, the surface albedo and scaling factors for stratospheric Aerosols. The tropospheric contribution parameter changes from elevation retrieval to tropospheric scaling after convergence for the elevation is reached. A correction for a possible wavelength misalignment is applied. The a priori is set to 300% for water vapour and, 30% for methane. The newly developed variable aerosol correction showed originally a bias to lunar occultation measurements. The bias could be corrected constraining the tropospheric aerosol amount during the retrieval procedure. This leads however to a slightly worse overall agreement with other reference data sets.
Additionally, several small modifications where applied between V3 and V3.0:

- Level 1 data versions V7.03 and 7.04 of SCIAMACHY are used instead of V6.03. The change of the satellite data version was necessary, because V6.03 is not provided for data newer than September 2010. The Differences between V6.03 and V7.03 include a small change in the calculation of instrument pointing and wavelength calibration. There are only minor differences between V7.03 and V7.04. The change was necessary because V7.03 does not exist after June 2006 and V7.04 was not reprocessed for the complete time series when the retrieval was started. The differences between the water vapour retrieved from Level 1 V7.03U compared to V7.04W are negligible, see Figure 11. Therefore data based on these different level 1 versions can be combined.
- European Centre for Medium range Weather Forecast (ECMWF) Interim reanalysis pressure and temperature fields are used in V3.0 instead of the analysis fields from ECMWF. The ECMWF reanalysis is calculated with a consistent model version while the model for the ECMWF analysis data changes frequently, e.g. in 2006 it was shifted to a finer vertical model grid. The effects of the change of data version and ECMWF fields showed only minor influence on the resulting water vapour profiles.
- The a priori for tropospheric contribution, surface albedo and stratospheric aerosol scaling are not replaced after each iterative step to achieve a faster convergence.

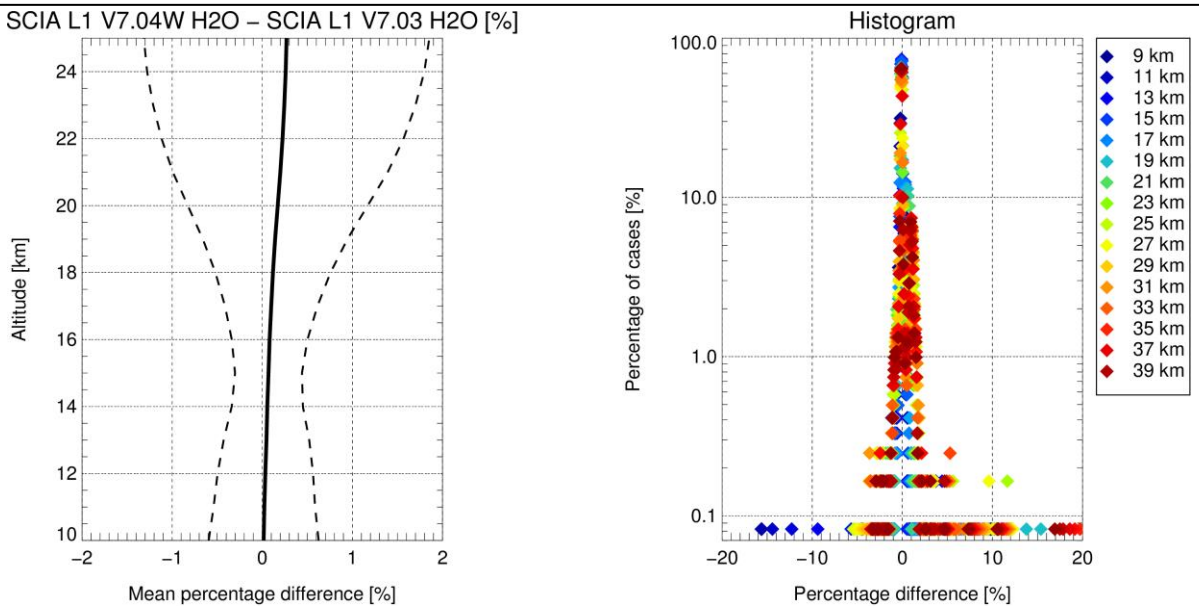

Figure 11: Mean relative difference and histogram of all differences between water vapour retrieved from level 1 version 7.03 consolidation U and 7.04W for 07., 15., and 23. February 2005, V3.01, 1236 profiles.

This version (V3.0) was processed for every 8th day globally. The data were filtered for clouds and measurements influenced by the South Atlantic Anomaly (SAA) prior to the retrieval. The cloud filter is based on the SCIAMACHY ClOud Detection Algorithm (SCODA) V1.9; see Rozanov et al., 2011. Retrieved profiles were further filtered for convergence, if the residua exceed 0.01. An example for the coverage of this data set during one month can be seen in Figure 12a, where the water vapour mixing ratios at 22 km altitude are shown for all profiles from July 2010.

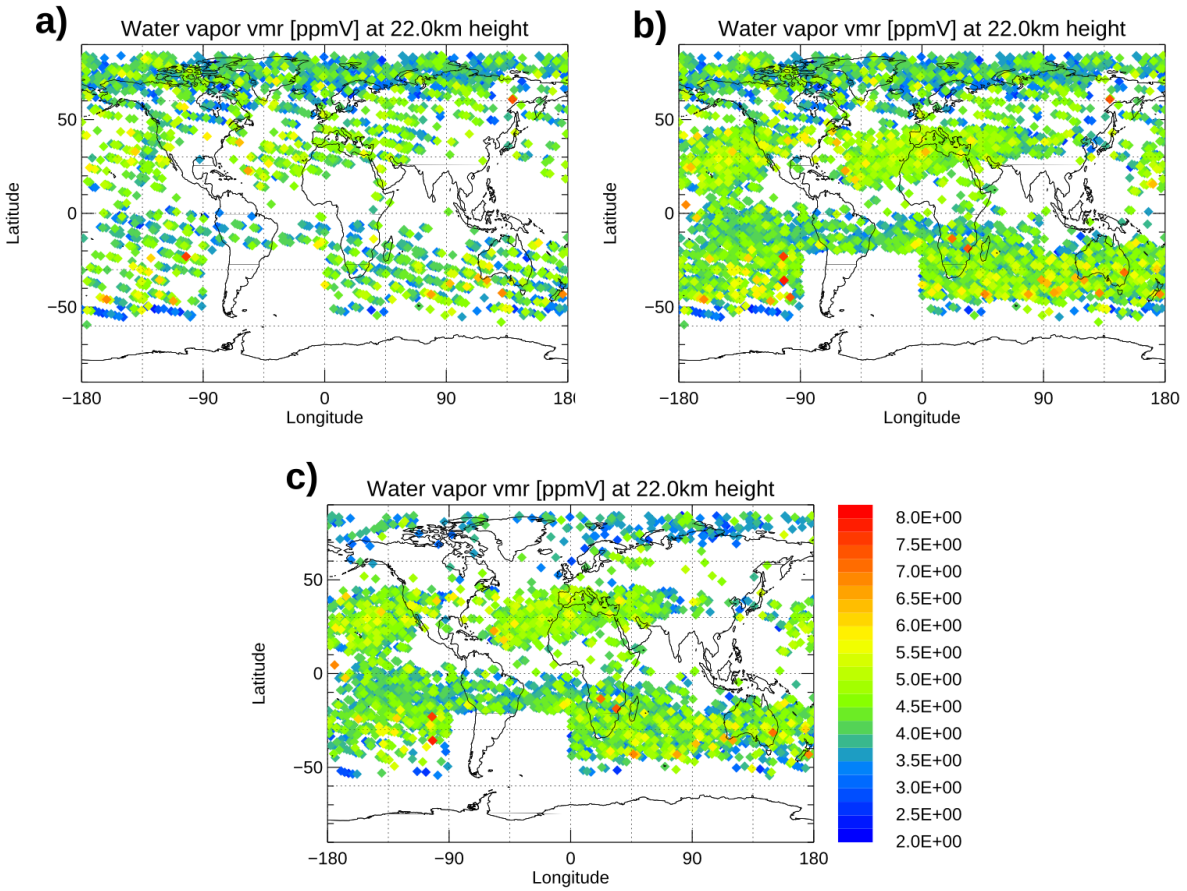

Figure 12: Water vapour volume mixing ratios [ppmV] from SCIAMACHY measurements in 22km altitudes. a) for every 8th day globally V3.0, b) for every 8th day globally, every second day between 45°S and 45°N, V3.0, c) as b) with resolution filter (V3.02).

Especially in the tropics large gaps exist between the profiles, because here high clouds are more probable. If clouds are observed above 10 km height a retrieval of the corresponding profile is not performed. For clouds up to 12 km height the retrieval is possible, using only the spectra measured above, but it was observed that the quality of these data and the probability that the retrieval converges is lower. Figure 13 shows the time series of V3.0 for every 8th day globally against altitude for 20°S-20°N and against latitude for 22 km height.

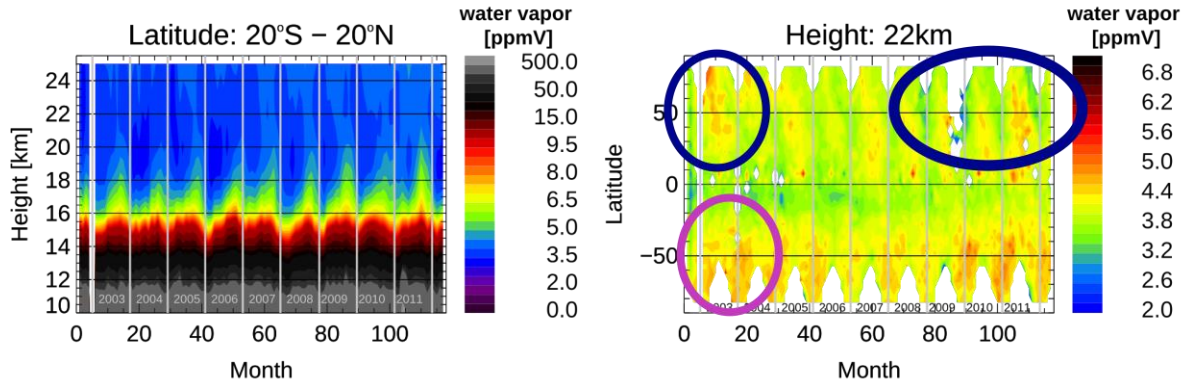

Figure 13: Time series of SCIAMACHY water vapour V3.0, every 8th day globally, averaged between 20°S and 20°N against height (left panel) and on a 5°x5° grid for an altitude of 22km against latitude (right panel).

2.2. Action plans to develop matured products

Further possibilities to improve the tropospheric aerosol correction were investigated but no substantial improvement could be reach. Therefore, we continued to process the existing version for the complete measurement period and for every second day between 45°S and 45°N. This region was chosen to obtain a better coverage where profiles are often not retrieved due to clouds and where the horizontal sampling is coarser due to the orbit geometry. The result for this higher sampling is shown for July 2010 in Figure 12b. The data set was tested for possible improvements by filtering for clouds and volcanic aerosols. A stricter filter was chosen, which excludes all profiles, where the retrieval does not converge (V3.01). Figure 14a shows the time series for this version. An additional resolution filter was tested, where profiles are excluded, if the resolution exceeds 8 km in the altitude range between 11 and 20 km or if the resolution is smaller or equal to zero (V3.02, see Figure 14b).

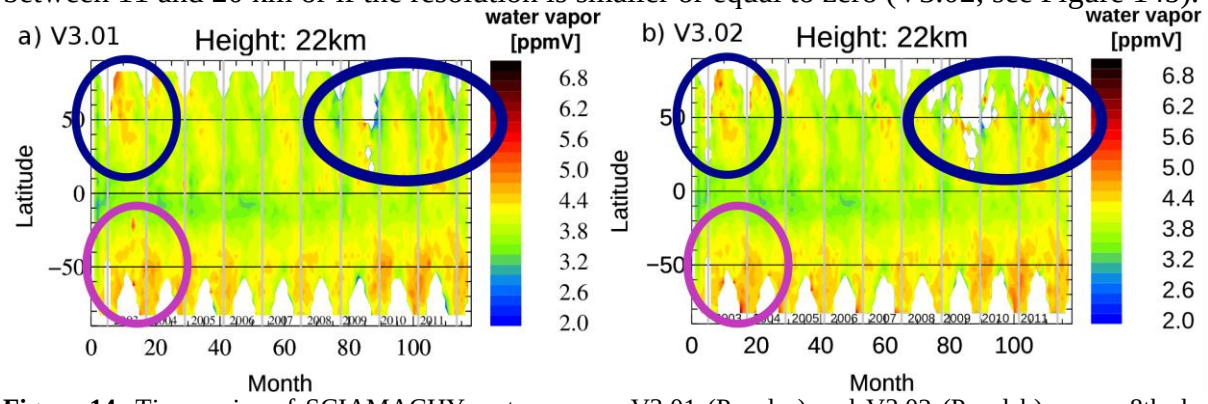

Figure 14: Time series of SCIAMACHY water vapour V3.01 (Panel a) and V3.02 (Panel b), every 8th day globally, every 2nd day between 45°S and 45°N on a 5°x5° grid for an altitude of 22km against latitude.

2.3. Characterisation of the matured product

The new filter decreased the number of profiles, especially in the Northern Hemisphere mid-latitudes and arctic, as can be seen from Figure 12c. Figure 14b shows the time series V3.02 for every 8th day globally and every second day between 45°S and 45°N against latitude, analogue to Figure 13 for the old sampling and filter.

The comparison to Figure 13 shows, that the time series got smoother and unrealistic high values in the tropic disappeared. The differences between the versions are usually not large and difficult to see in the 2D plots. Blue circles mark, where the coverage is different between the data versions. The pink circle marks a region with relatively large differenences in the structures. In the second half of 2009, more data are missing in Northern Hemisphere, where an influence of aerosols from the volcanic eruption of Sarychev can be expected. To get a more detailed view on the quality of the matured data product, Figure 15 shows the mean profiles and standard deviation for the collocated profiles and their mean percentage difference between V3.02 and MLS data V3.3. The collocation criteria are less than 100 km distance, 6h time difference and a criterion for the modified potential vorticity (MPV) at 475K (less than 3PVU difference, no profiles between 30 and 40PVU for all data polewards of 35° Latitude). See a more detailed description and comparisons for different regions in the product validation report.

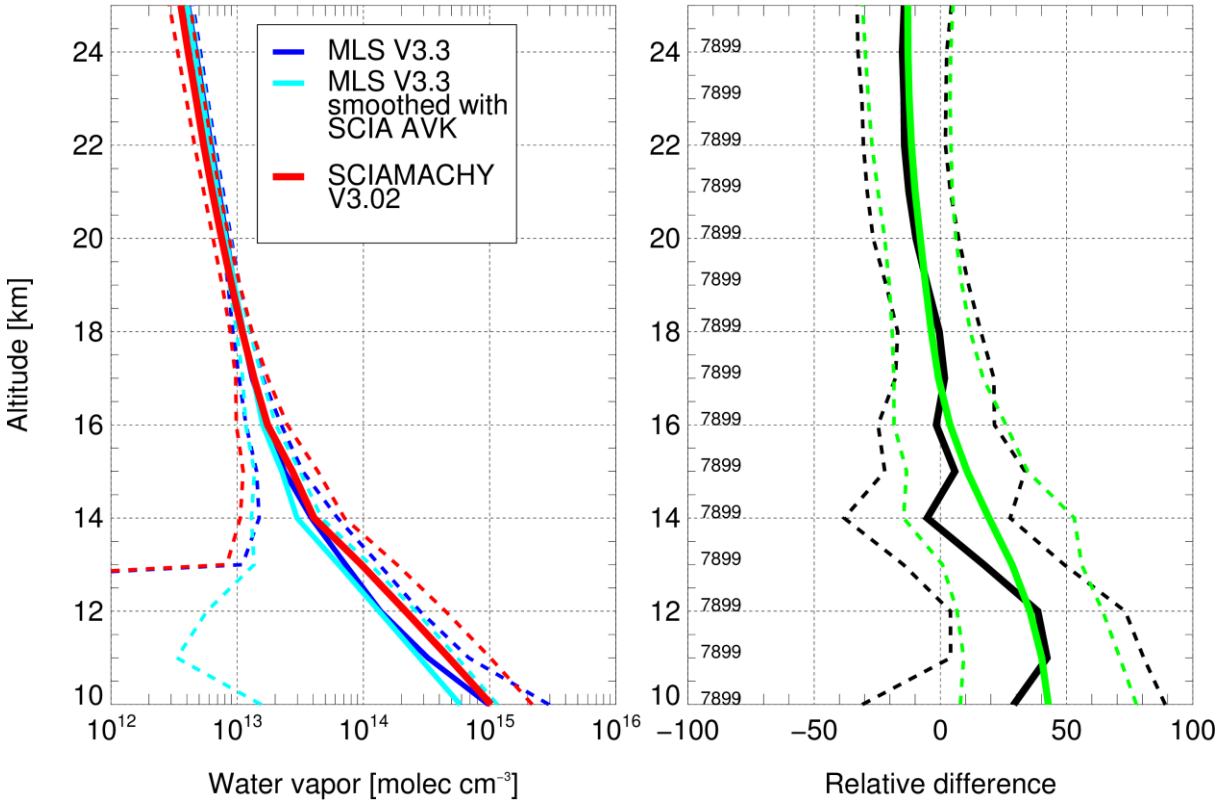

Figure 15: Comparison between collocated water vapour profiles of SCIAMACHY V3.02 and MLS V3.3. Left panel: mean collocated profiles and standard deviation in number density, right panel: mean percentage difference with (green) and without (black) smoothing of the MLS data with the SCIAMACHY AVK. The number of collocations in indicated in the right panel for each altitude.

Above 18km the SCIAMACHY profiles show dryer values than the MLS data (10-15% difference), below 14km the MLS data are dryer (up to 45% difference). Figure 16 shows the same comparison without the resolution filter (V3.01). The number of collocations found is much higher in this case, but also the standard deviation of the SCIAMACHY data is larger than the one of the MLS data while they are comparable if the resolution filter is applied. Generally, the SCIAMACHY data are dryer without resolution filter. Therefore the mean percentage difference to the MLS water vapour increases above about 16 km and decreases below.

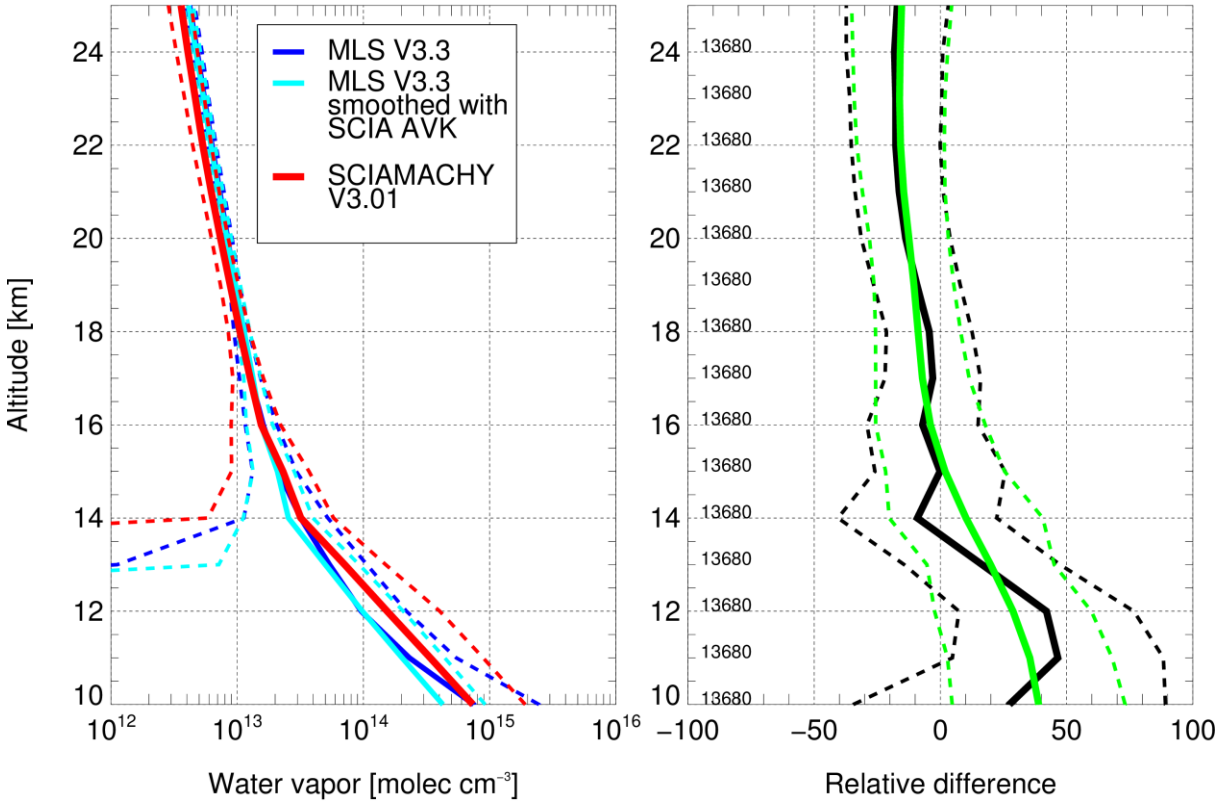

Figure 16: As Figure 15 without resolution filter (V3.01).

Figure 17 shows a comparison between the time series of collocated profiles averaged globally to 30 day bins for selected altitudes with and without resolution filter. As for the profile, the resolution filter increases the difference for the time series at 12 and 15km and decreases it for 18 and 22 km altitude. There is no clear drift compared to MLS for the two higher altitudes. The difference seems to increase for the two lower altitudes. Also for data with and without resolution filter larger differences occur from 2008 on. Generally, the resolution filter removes probably too many profiles in the mid and high latitudes. High resolution values can indicate a reduced data quality, but occur also, if the lowest two measurement altitudes are separated by more than 3.3km due to refraction and one retrieval grid point is located exactly between them. In these cases the resolution indicates that the retrieval grid is too dense for the vertical sampling of the measurements. This result for these profiles is often acceptable; the effected altitudes are then rather an interpolation of the water vapour below and above. Therefore, both V3.01 and 3.02 are provided.

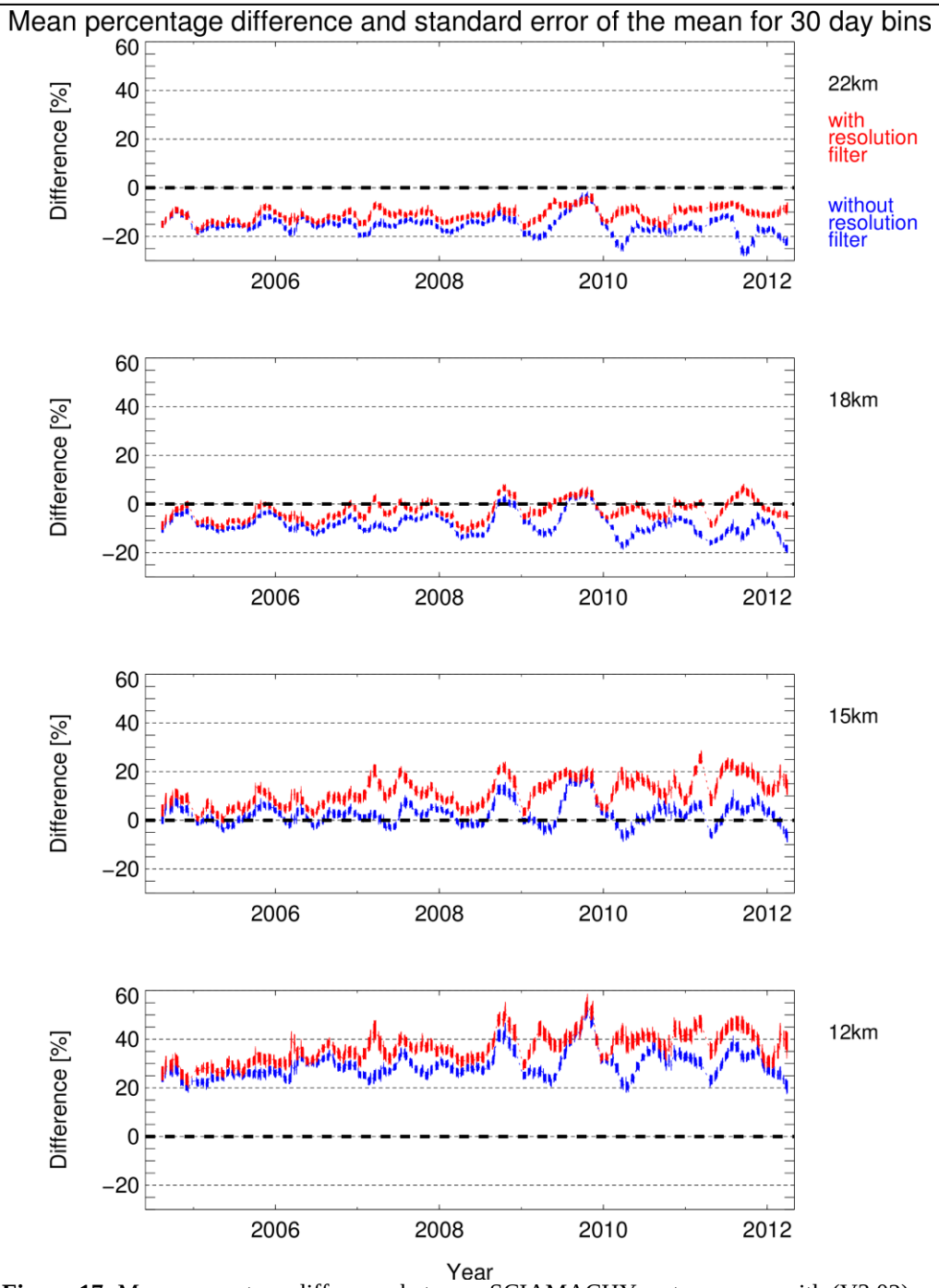

Figure 17: Mean percentage difference between SCIAMACHY water vapour with (V3.02) and without (V3.01) resolution filter and MLS V3.3 for globally averaged 30 day bins.

3. WP 15: Evaluation of SPARC Data Initiative climatologies

3.1. Status of the products

Table 1 lists all ESA, ESA-third party and other space agencies' trace gas and aerosol zonal mean monthly mean climatologies submitted to the SPARC Data Initiative as of June 2012. The SPARC Data Initiative climatologies span the time period from 1978-2010 and the height range 300-0.1 hPa, with focus on the stratosphere. The earliest ESA and ESA-third party missions start in 2003. The available altitude coverage is dependent on trace gas species and

instrument (for details we refer to the SPARC Data Initiative report). The level-2 data versions from the different instruments that were used to produce the level-3 products for the SPARC Data Initiative are specified in Table 2.

Table 1: Overview of SPARC Data Initiative climatologies of different chemical trace gas and aerosol observations listed by instruments. ESA and ESA-third party instruments are indicated in blue, all other instruments in grey.

	O_3	H_2O	CH_4	N_2O	CCl_3F	CCl_2F_2	CO	HF	SF_6	NO	NO_2	NO_x	HNO_3	HNO_4	N_2O_5	$ClONO_2$	NO_y	HCl	ClO	HOCl	BrO	OH	HO_2	CH_2O	CH_3CN	aerosol
GOMOS	x										x															x
MIPAS	x	x	x	x	x	x	x		x	x	x	x	x	x	x	x	x		x	x				x		
SCIAMACHY	x	x									x	x_d									x					x
ACE-FTS	x	x	x	x	x	x	x	x	x	x	x	x	x	x	x	x	x	x						x		
MAESTRO	x																									
OSIRIS	x										x	x_d					x_m				x					x
Odin/SMR	x	x		x			x			x			x				x_m		x					x_{lc}		
POAM II	x										x															x
HALOE	x	x	x					x		x	x	x						x								
HIRDLS	x				x	x					x		x													
LIMS	x	x									x		x													
POAM III	x	x									x															x
SAGE I	x																									
SAGE II	x	x									x															x
SAGE III	x	x									x															x
SMILES	x												x					x	x	x	x		x		x	
Aura-MLS	x	x		x			x						x					x	x	x		x	x			
UARS-MLS	x	x											x						x							

Table 2: Overview of data versions from ESA and ESA-third party instruments that were used to compile the SPARC Data Initiative climatologies.

	GOMOS ESA operational processor	**MIPAS** (2002-2004) IMK/IAA L2	**MIPAS** (2005-2010) IMK/IAA L2	**SCIAMACHY**	**ACE-FTS**	**ACE-MAESTRO**	**Odin/SMR**	**OSIRIS**
O_3	V5	V3o_O3_9	V4o_O3_202	V2.5	V2.2	V1.1	V2.1	V5
H_2O	---	V3o_H2O_13	V4o_H2O_203	V3.0	V2.2	---	V2.1	---
CH_4	---	V3o_CH4_11	V4o_CH4_201	---	V2.2	---	---	---
N_2O	---	V3o_N2O_11	V4o_N2O_201	---	V2.2	---	V2.1	---
HNO_3	---	V3o_HNO3_9	V4o_HNO3_201	---	V2.0	---	V2.0	---
NO_2	V5	V3o_NO2_14	V4o_NO2_200	V3.1	V2.2	---	---	V3
NO	---	V3o_NO_14	V4o_NO_200	---	V2.2	---	V2.1	---
N_2O_5	---	V3o_N2O5_10	V4o_N2O5_200	---	V2.2	---	---	---
HNO_4	---	V3o_HNO4_12	V4o_HNO4_200	---	V2.2	---	---	---
$ClONO_2$	---	V3o_ClONO2_12	V4o_ClONO2_201	---	V2.2	---	---	---
ClO	---	V3o_ClO_11	V4o_ClO_200	---	---	---	V2.1	---
HOCl	---	V3o_HOCl_4	---	---	---	---	---	---
CCl_3F	---	V3o_CFC11_10	V4o_CFC11_200	---	V2.2	---	---	---

	GOMOS ESA operational processor	**MIPAS** (2002-2004) IMK/IAA L2	**MIPAS** (2005-2010) IMK/IAA L2	**SCIAMACHY**	**ACE-FTS**	**ACE-MAESTRO**	**Odin/SMR**	**OSIRIS**
CCl_2F_2	---	V3o_CFC12_10	V4o_CFC12_200	---	V2.2	---	---	---
HCl	---	---	---	---	V2.2	---	---	---
CH_2O	---	V3o_H2CO_1	---	---	---	---	---	---
BrO	---	---	---	V3.2	---	---	---	V5
HO_2	---	---	---	---	---	---	V2.1	---
CO	---	V3o_CO_12	V4o_CO_200	---	V2.2	---	V2.1	---
SF_6	---	---	V4o_SF6_201	---	V2.2	---	---	---
HF	---	---	---	---	V2.2	---	---	---
aerosol	V5	---	---	V1.0	---	---	---	V5

3.2. Product accuracy and error characterization

The accuracy and error characterization of the different chemical trace gas and aerosol level-2 data used for the compilation of the SPARC Data Initiative climatologies is listed in Tables 3-9. The numbers refer to the stratosphere, the focus of the SPARC Data Initiative. The most important trace gas species that are available for most instruments are marked with colour for better comparability. The tables also list references, in which more information on the validation approach and data products can be found. Note however, that the listed uncertainties are not necessarily comparable among the different instruments, since error characterization methods are usually not applied consistently among the instrument teams. Also, the listed uncertainties are not to be mistaken for the uncertainties in the SPARC Data Initiative climatologies. The averaging over multiple profiles in one climatology grid cell will greatly remove the random error of a single profile (and also the error derived from the average of a limited number of coincident profiles). On the other hand, the climatology uncertainties will include in addition to measurement biases related to retrieval errors, errors in input parameters of the retrieval (e.g., spectroscopic data), and smoothing errors related to the resolution of the measurements, biases introduced through temporal and spatial sampling, and differences in averaging techniques during the compilation of the climatologies. The SPARC Data Initiative report will provide information on this overall uncertainty of the climatologies by using a top-down, empirical approach to estimate the error and uncertainty of the different trace gas and aerosol climatologies. This information is however not yet available and will be published in the SPARC Data Initiative report by the end of 2013.

Table 3: Error characterization of GOMOS level-2 data products used to compile the SPARC Data Initiative climatologies. GOMOS accuracy is determined from geophysical validation and study of model errors. GOMOS error/precision is obtained via error estimates. Note, GOMOS precision has worsened during its lifetime because of increased dark current noise. Also, individual errors depend on the occulted star's visual magnitude and effective temperature. For example, very cool and weak stars cannot support ozone retrievals above 40 km.

Species	**Accuracy**	**Precision**	**Reference**
O_3	2%	0.5-5%	Sofieva et al. (2009); Tamminen et al. (2010); Bertaux et al. (2010)
NO_2	within 10%	10-20%	Hauchecorne et al. (2005); Tamminen et al. (2010); Bertaux et al. (2010)

Aerosol	within 20%	10-50%	Tamminen et al. (2010); Bertaux et al. (2010); Vanhellemont et al. (2010)

Table 4a: Error characterization of MIPAS (2002-2004) level-2 data products used to compile the SPARC Data Initiative climatologies. The comment includes information on the validation approach used. Errors are given in units of vmr or in percentage numbers, whichever leads to a smaller dynamic range of error estimates (they vary considerably with altitude).

Species	Accuracy	Precision	Reference
O_3	3-10%	5-10%	Steck et al. (2008)
H_2O	6-18%	5-10%	Milz et al. (2009)
CH_4	4-20%	5-10%	Glatthor et al. (2005)
CO	8-15%	15-40%	Funke et al. (2009)
N_2O	2-14%	8-15%	Glatthor et al. (2005)
NO	<15%	~10%	Funke et al. (2005; 2011)
NO_2	<10%	5-10%	Funke et al. (2005; 2011)
HNO_3	4-40%	6-53%	Mengistu Tsidu et al. (2005)
N_2O_5	10-20%	10-100ppt	Mengistu Tsidu et al. (2005)
HNO_4	15%	25%	Stiller et al. (2007)
$ClONO_2$	5%	60-100ppt	Hoepfner et al. (2004; 2007)
ClO	5-25%	50-400ppt	Glatthor et al. (2004)
HOCl	10%	30-80ppt	von Clarmann et al. (2012)
CCl_3F	10%	5-28%	Kellmann et al. (2012)
CCl_2F_2	10%	20ppt	Kellmann et al. (2012)
CH2O	8%	70-115ppt	Steck et al. (2008)

Table 4b: Same as Table 4a, but for MIPAS (2005-2010) level-2 data products.

Species	Accuracy	Precision	Reference
O_3	~11%	4-12%	von Clarmann et al. (2009); Stiller et al. (2012)
H_2O	6-18%	5-8%	von Clarmann et al. (2009); Stiller et al. (2012)
CH_4	10-20%	5-9%	von Clarmann et al. (2009)
CO	N/A	15-40%	validation not completed, but similar to table 4.4a
N_2O	4-11%	5-10%	von Clarmann et al. (2009)
NO	N/A	~10%	validation not completed, but similar to table 4.4a
NO_2	N/A	5-10%	validation not completed, but similar to table 4.4a
HNO_3	2-9%	2.5-17%	von Clarmann et al. (2009)
N_2O_5	N/A	N/A	validation not completed
HNO_4	N/A	N/A	validation not completed
$ClONO_2$	5%	23-105ppt	von Clarmann et al. (2009)
ClO	10-40%	200-600ppt	von Clarmann et al. (2009)
CCl_3F	10%	4-35%	Kellmann et al. (2012)
CCl_2F_2	10%	22-28ppt	Kellmann et al. (2012)
SF_6	6%	10-40%	Stiller et al. (2012)

Table 5: Error characterization of SCIAMACHY level-2 data products used to compile the SPARC Data Initiative climatologies. The comment includes information on the validation approach used. The precision here is defined as the total error (i.e., sum of the noise and smoothing errors of the retrieval).

Species	Region	Accuracy	Precision	Reference
O_3		within 10%	10-20%	from N. Rahpoe (pers. comm., Ozone_CCI project)
H_2O	above 14 km	10-15%	10-20%	Rozanov et al. (2011)
NO_2	above 20 km	10-20%	10-20%	Bauer et al. (2012)

BrO	mid/high lats tropics	15-20% ~30%	30-50%	Rozanov et al. (2011)
Aerosol		20-30%	N/A	Ernst et al. (2012)

Table 6: Error characterization of ACE-FTS level-2 data products used to compile the SPARC Data Initiative climatologies. The comment includes information on the validation approach used. The error characterization was based on coincident measurements, except for CFC-11 and CFC-12, for which zonal means were used.

Species	Region	Accuracy	Precision	Reference
O_3	~16-44 km	+1 to +8%	N/A	Dupuy et al. (2009)
H_2O	15-70 km	< 5-10%	N/A	Carleer et al. (2008)
CH_4	lower strato upper strato	within 10% up to 25%	N/A	Mazière et al. (2008)
CO	lower strato 30-100 km	< 30% < 25%	N/A	Clerbaux et al. (2008)
N_2O	18-30 km 30-60 km	within ±10 ppbv +1 to -2 ppbv	N/A	Strong et al. (2008)
NO	22-64 km	±8% (average)	N/A	Kerzenmacher et al. (2008)
NO_2	25-40 km	within 20% from	N/A	Kerzenmacher et al. (2008)
HNO_3	18-35 km	better than ±20% (typically ±10%)	N/A	Wolff et al. (2008)
N_2O_5	16-27 km	-10% (daytime) -27% (nighttime)	N/A	Wolff et al. (2008)
HNO_4	N/A	N/A	N/A	validation not completed
$ClONO_2$	16-27 km 27-34 km	±1% > +14%	N/A	Wolff et al. (2008)
CCl_3F	7-20 km	±20%	N/A	Mahieu et al. (2008)
CCl_2F_2	7-25 km	±20%	N/A	Mahieu et al. (2008)
HCl			N/A	Mahieu et al. (2008)
SF_6	N/A	N/A	N/A	validation not completed
HF	20-50 km	5-10%	N/A	Mahieu et al. (2008)

Table 7: Error characterization of ACE-MAESTRO level-2 data products used to compile the SPARC Data Initiative climatologies. The comment includes information on the validation approach used.

Species	Region	Accuracy	Precision	Reference
O_3	~18-44 km 45-55 km	±6% (average) +10 to +30%	N/A	Dupuy et al. (2009)

Table 8: Error characterization of Odin/SMR level-2 data products used to compile the SPARC Data Initiative climatologies. Note that the accuracy here has to be interpreted as systematic error and was usually estimated for earlier SMR data versions.

Species	Region	Accuracy	Precision	Reference
O_3	12-50 km	<0.75 ppmv	1.5 ppmv	Urban et al. (2006)
H_2O	20-75 km	N/A	<1 ppmv	Urban et al. (2005)
CO	20-110 km	N/A	N/A	validation not completed
N_2O	>30 km <30 km	<12 ppbv	<30 ppbv 10-15%	Urban et al. (2006)
NO	30-70 km	N/A	N/A	validation not completed
HNO_3	>30 km <30 km	<0.7 ppbv	<1 ppbv 10-30%	Urban et al. (2006)
HO_2	30-60 km	N/A	<0.5 ppbv	Khosravi et al. (2012)
ClO	15-50 km	0.1 ppbv	0.15 ppbv	Urban et al. (2006)

Table 9: Error characterization of OSIRIS level-2 data products used to compile the SPARC Data Initiative climatologies. The comment includes information on the validation approach used. For BrO, the validation has been performed on daily zonal mean data. For aerosol, the accuracy is estimated for high latitudes only.

Species	Accuracy	Error/ precision	Reference
O_3	2%	4%	Degenstein et al. (2009); Bourassa et al. (2011)
NO_2	20%	10%	Haley et al. (2004); Brohede et al. (2007)
BrO	30%	30%	McLinden et al. ()
Aerosol	10%	15%	Bourassa et al. (2012) Bourassa et al. ()

3.3. Action plans to develop matured products

The goal of the SPARC Data Initiative is that its level-3 climatologies will be updated and uploaded onto the SPARC Data Center website whenever the instrument teams have developed and validated new level-2 data versions. This will keep the SPARC Data Initiative climatology archive a dynamic database and ensure that the uncertainty of the climatologies is decreasing over time. More detailed and instrument-specific recommendations on how the quality of the different data products should be improved will follow from the SPARC Data Initiative Report.

4. WP 16: Short-lived species climatologies

4.1. Status of the products

A variety of short-lived species climatologies has been produced within the SPARC data initiative. These monthly zonal mean trace gas climatologies were calculated using 5^o latitude bins on a pressure grid with 28 levels between 300 and 0.1 hPa. An overview of the SPARC-DI climatologies is given in Section 3.

WP-16 focuses on the improvement of selected climatologies from the Odin satellite, namely those for the short-lived species ClO, NO, NO_2, and HNO_3, and consequently those for the derived chemical families NO_x ($NO + NO_2$) and NO_y ($NO_x + HNO_3 + ClONO_2 + N_2O_5$). The sun-synchronous near-terminator Odin orbit is not stabilized and a slow (non-linear) drift in altitude (between about 620km to 580km) and of the equator crossing time (between 6 and 7 am/pm) has occurred over the course of the mission. This leads to a slow variation of the local solar time of the measurements over the mission. Moreover, yaw manoeuvres, executed during special campaigns or on a more regular seasonal basis for extending the spatio-temporal range of the Odin measurements, lead to a large variability of the local solar time of the measurements. Figure 18 shows the local time of the Odin/SMR observations for a standard measurement mode.

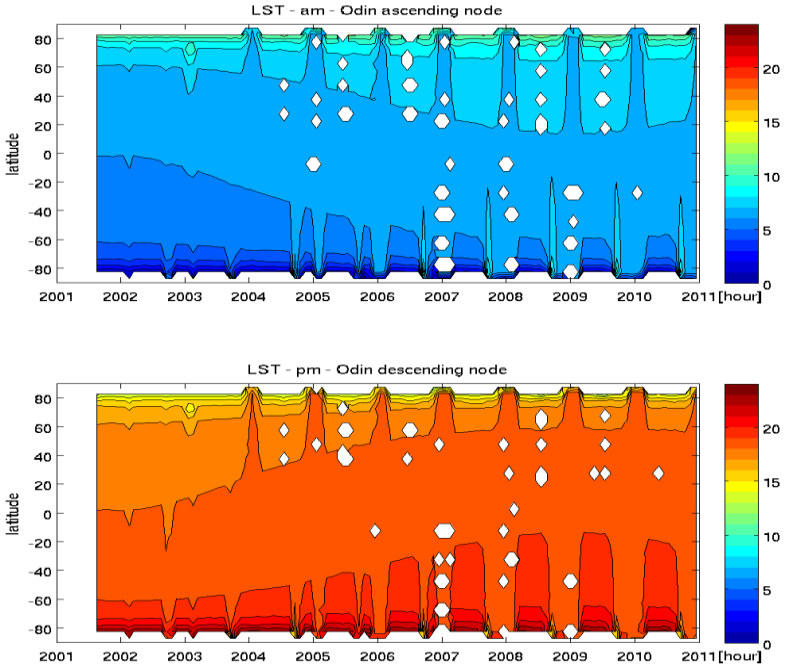

Figure 18: Local solar time of Odin/SMR measurements for the standard stratospheric measurement mode. Top: ascending node (am). Bottom: descending node (pm).

For species with large diurnal variations it is therefore essential to (1) separate measurements at the ascending and descending nodes and to (2) produce additional climatologies using a photochemical box model to scale the measurements to a common local solar time in order to enable direct comparisons between products from different instruments with different spatio-temporal sampling patterns. Scaled climatologies of species of the NO_y family (NO, NO_2) have therefore been calculated for 10am and 10pm, the approximate local time of the Envisat/MIPAS measurements. In contrast, the ClO measurements were scaled to 1:30am and 1:30pm which is the approximate local time of the Aura-MLS measurements between about 60S to 60N.

4.2. Product accuracy and error characterization

Table 8 summarizes the errors of Odin/SMR level-2 data products used to compile the SPARC Data Initiative climatologies and Table 9 gives corresponding information for Odin/OSIRIS. An evaluation of the relevant short-lived species (ClO, NO, NO_2, HNO_3) is undertaken within the SPARC data initiative by comparison to independent measurements of

Aura/MLS and Envisat/MIPAS, among many others sensors. This work has not been completed at the time of writing of this report (see Section 3). For trend analysis based on the matured products developed within SPIN, it is furthermore possible to check the internal consistency of the Odin climatologies with respect to long term changes by comparing scaled am and pm time-series.

4.3. Action plans to develop matured products

As explained earlier in Section 3, the goal of the SPARC Data Initiative is that its level-3 climatologies will be updated and uploaded onto the SPARC Data Center website whenever the instrument teams have developed and validated new level-2 data versions. The SPIN short-lived species climatologies will thus be uploaded to the SPARC data center once the products have been verified and documented. The data analysis plan to develop matured products is as follows:

1) Data inter-comparisons (quality assessment) and selection of promising "candidates": ClO, NO, NO_2, HNO_3.
2) Correction methods for SZA dependence of species concentrations: Scaling with help of model look-up tables.
3) Model optimization (initialisation) and scaling factor look-up table computation.
4) Construction of unscaled/scaled monthly zonal mean climatologies.
5) Quality assessment:
    1. Intercomparison of scaling factors from PRATMO and MISU-1D models (Uncertainties? Validity range in terms of latitude and pressure?).
    2. Assessment of validity range and limitations of the climatologies.
    3. Internal am/pm consistency of time evolution.
    4. Comparisons with external satellite data sets: inter-comparison / assessment of SPARC-DI and updated SPIN scaled climatologies for ClO, NO_2, NO, HNO_3.
6) Calculation of chemical families NO_x and NO_y.
7) Documentation of results.

4.4. Characterisation of the matured products

1) Odin short-lived species data have been compared to several other observational data sets. Khosravi et al. (ACP-2013) recently published a systematic comparison of SMR measurements of ClO and HO_2 with observations from JEM/SMILES and Aura/MLS. Results of these inter-comparisons, based on a local time sensitive method, are summarised in the SPIN Product Validation Report. HO_2 was measured by SMR only during a one year period from October 2003 to October 2004 owing to a instrumental (frequency stability) problem with the 576GHz radiometer. In contrast, the SMR ClO data sets spans now a period from November 2001 to present (February 2014). The data set has already earlier been used for trend analyses in the tropical upper stratosphere using a simple scaling correction for the local time effect (Jones et al. ACP-2011) and the SPARC-DI climatologies have been refined as part of the SPIN project. Comparisons of Odin short-lived species such as ClO, NO_2, HNO_3, and NO with correlative measurements have been published earlier (e.g. Livesey, MLS-quality- document-2013; Brohede et al., CJP-2007; Wolff et al., JGR-2008; ...). Given the good quality and the long period covered by the data sets, the SPARC-DI climatologies of these species have been refined and extended.
2) Correction methods for the solar zenith angle dependence of species concentrations have been reviewed. The only practical solution is to prepare climatological look-up

tables of scaling factors derived from an appropriately initialised 1d photo-chemical model. Only for OSIRIS, SPARC-DI NO_2 scaling factors were calculated for each separate profile measurement, i.e. the model was constraint with the OSIRIS profile measurements of ozone and appropriate temperature / pressure information.

3) Scaling factors can be derived for any reference and measurement local time from look-up tables based on model calculations. The model (MISU-1d) has been run for the latitudes between 90°S to 90°N with a step of 5°, for altitudes from 15 to 70 km with a resolution of 1km and for one day per month during one year. Model results are stored for one complete diurnal cycle from each individual model run and for each species. The model was initialised using zonal mean temperatures and pressures calculated from ECMWF analyses, a water zonal mean climatology derived from Aura/MLS measurements, and ozone zonal mean fields from the CMAM model. NO_y was constrained to values taken from an ACE-FTS climatology and Cl_y was constrained according to Nassar et al. (2006). Note that a chemical box model cannot consider all effects such as diurnal effect produced by a diurnal variation in temperature which alters the chemical equilibrium. Use of a Chemical Transport Model (CTM) based on prescribed meteorological data could be an improvement but requires considerably larger computational ressources. Also, the good agreement of the modelled diurnal cycles by the 1d model with observed diurnal variation of ClO, HOCl, and HO2 by SMILES [Khosravi et al., 2013] indicates that the 1d model can be employed for local time scaling of short-lived species with strong photolysis dominated diurnal cycle, such as for the here relevant species ClO, NO, NO2.
4) Morning and evening data were used to separately calculate am and pm monthly zonal mean climatologies as this is the common procedure for SPARC-DI short-lived species. The monthly zonal mean data sets were hereby extended in time as the SPARC-DI data sets typically end in 2010. Scaling factors from the model look-up table were used to additionally calculate scaled monthly zonal mean climatologies with reference time 1:30am and 1:30pm for ClO and 10am and 10pm for NO_y species.
5) Quality assessment:
    1. As an initial step, an inter-comparison of scaling factors from the PRATMO and MISU-1d models has been undertaken (see Figure 19). It turns out that differences are largest for observations close to the terminators at about sunrise and sunset (Odin in the tropics), but differences remain between about 0.1-0.2. The smallest differences between the scaling factors from MISU and PRATMO were found for night and day time observations (Odin at middle and high latitudes in the winter and summer hemispheres, respectively). Less good agreement was found for scaling factors at the highest latitudes (80°N and 80°S). The differences are still within 0.15 and 0.2, but a different shape of ClO diurnal variation is calculated by the models. To conclude, largest differences between model scaling factors indicate an upper limit of the systematic error of about 20% arising from the model and its initialisation.
    2. Assessment of validity range and limitations of the climatologies (see Figure 21). Work has been undertaken for ClO and NO with the aim of optimising the applied methodology in terms of data filtering: better reference time for scaling is 1:30 am (night-time), whilst scaling to 1:30 pm results in too large ClO in the winter hemisphere requiring filtering. Results indicate that scaling factors should be smaller than 5 for the climatologies scaled to 1:30pm in the afternoon or 1:30am in the morning. The zonal mean fields of the model scaling factors are stored in the climatology files and more stringent criteria can therefore be specified for sensitive

applications such as trend analysis. The polar winter regions below about 30km (latitudes poleward of 60°) have to be excluded as the model computed scaling factors are only valid for gas phase chemistry.

3. Internal am/pm consistency of the time evolution. An internal verification of the method and the resulting scaled ClO climatologies is done by comparison of scaled am and pm ClO time-series for various altitude and latitude bands. This is shown in Figure 22 for the 3hPa level in the tropics (20S-20N). Differences in the time evolution of the am and pm zonal mean climatologies have been accounted for in the scaled am and pm climatologies which show both nearly the same time evolution. Future trend studies for ClO will rely on such successfully scaled am and pm zonal mean data sets.

6) Verification with external satellite data sets is based on inter-comparison / assessment of SPARC-DI and updated SPIN scaled climatologies for ClO, NO2, NO, and HNO3. The finalised Odin climatologies, matured within SPIN, will be uploaded on the SPARC-DI data server upon completion of the optimisation work. A publication in the peer-reviewed literature describing the data sets in detail is planned. Moreover, a description of the data sets will also be included in the SPARC-DI final report.

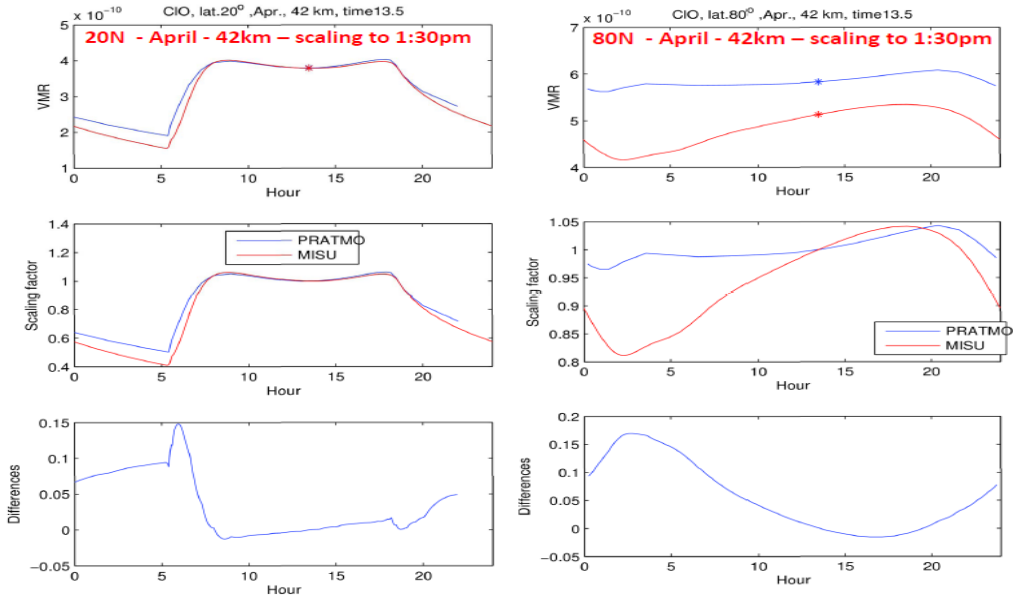

Figure 19: Comparison of MISU-1d and PRATMO photochemical models (top) and derived scaling factors (middle) for ClO. Left: latitude 20N, 42.5km, April. Right: same but for 80N. In this example scaling factors were calculated for a reference time 1:30pm. The differences of the scaling factors are shown in the bottom row.

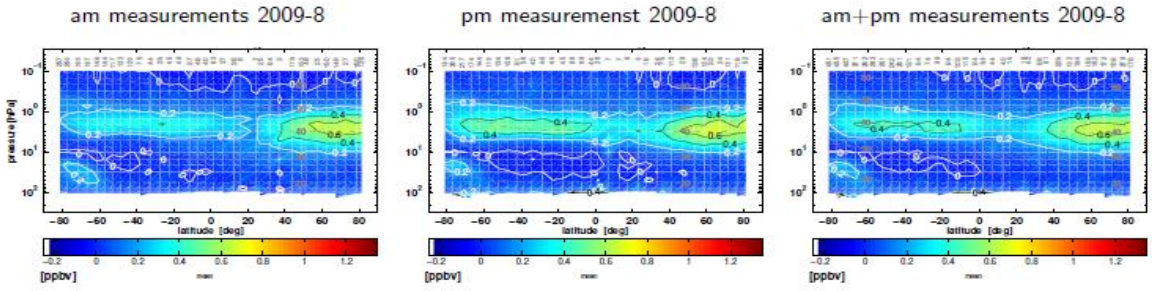

Figure 20: Odin/SMR ClO zonal monthly mean for am (left), pm (middle) and all measurements (right) August 2009 (from Khosravi et al. 2013b).

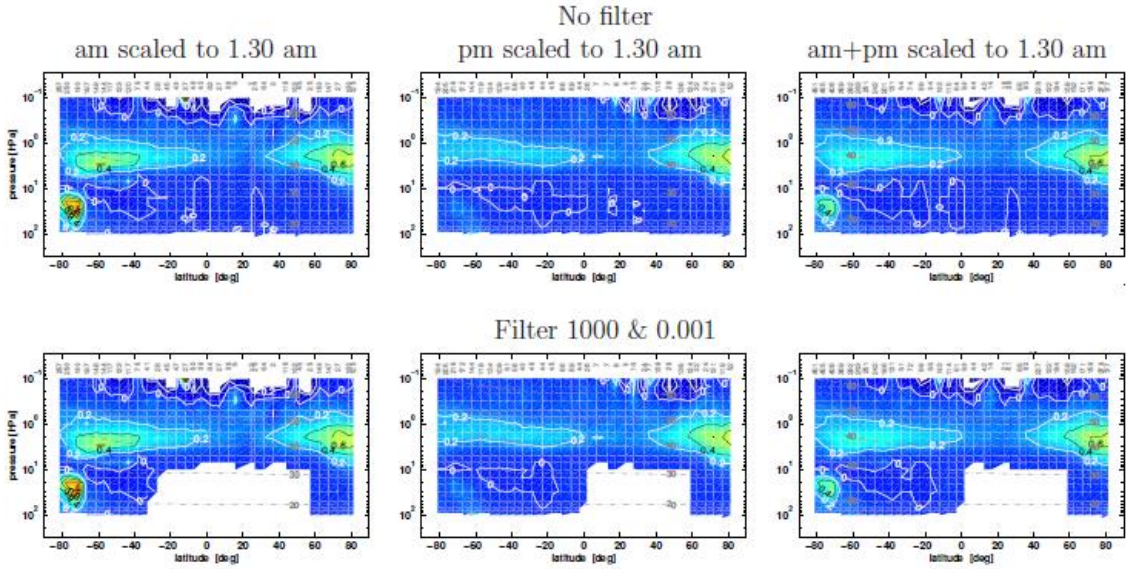

Figure 21: Odin/SMR ClO monthly zonal mean of August 2009 scaled to 1.30am. Top: The figures (from left to right) represent a.m. observations scaled to 1.30 a.m., p.m. observations scaled to 1.30 a.m., and all observations scaled to 1.30 a.m. Bottom: Same as top row, but data with scaling factors larger than 1000 or smaller than 0.001 have been filtered out (from Khosravi et al. 2013b).

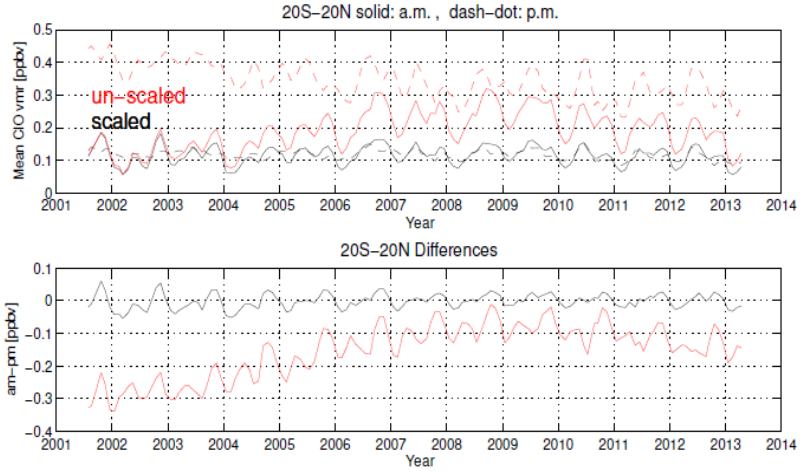

Figure 22: Top row: Odin/SMR ClO observations as a function of time for 20°S–20°N and the 3 hPa pressure level. A.m. and p.m. monthly averages are shown as solid and dashed lines, respectively. Red: non-scaled time-series. Black: time-series for ClO scaled to 1.30 a.m.. Bottom row: Differences between a.m. and p.m. observations for both scaled and non-scaled ClO time-series, indicating the improvement in terms of long-term drifts achieved through model assisted local time scaling (from Khosravi et al., 2013b).

5. WP 17: GOMOS bright limb algorithm and sample processing

5.1. Status of the products

The GOMOS bright limb (GBL) Level 2 data set has been created. The GBL data set consists of 323000 stratospheric ozone profiles measured between 2002-2012. The profiles are retrieved in the 20-60 km altitude range and have approximately 2-3 km vertical resolution. The current version of the data is 1.1 and the size of the total data set is about 20 GB. The files are in the standard HDF5 format. The files are available from the ftp.fmi.fi server with the username **gomosGBL** and the password **kOs20mos!**.

It should be noted that, in addition to the ozone profiles, the GBL files also include retrieved aerosol and neutral air number density profiles. The quality of these additional products is not determined within this project. The accuracy of the GBL aerosol product is not expected to be very good because the retrieval is optimized for ozone.

5.2. Product accuracy and error characterization

We have performed an initial validation for the GBL ozone product. The comparison against GOMOS night occultations (bright and hot stars) suggest that the bias of the GBL ozone is less than 10 % between 20 and 55 km except the 35-42 km range where the GBL profiles have a clear 10-18 % negative bias (depending on the latitude). There is also up to 30 % positibe bias in the 50 km tangent height at high latitudes. See Figure 23 and the product validation report for additional information. The collocation criteria was <250 km and <24 h against GOMOS night occultations and <200 km and <12 h against MLS.

The GBL ozone profiles include error estimates but they are not exactly precise in this first version of the product. The error estimate of the radiance is too large due to incorrect error of the dark charge. This leads to chi-square values less than one and slightly too pessimistic error bars. The error bars will be corrected in the next GBL version.

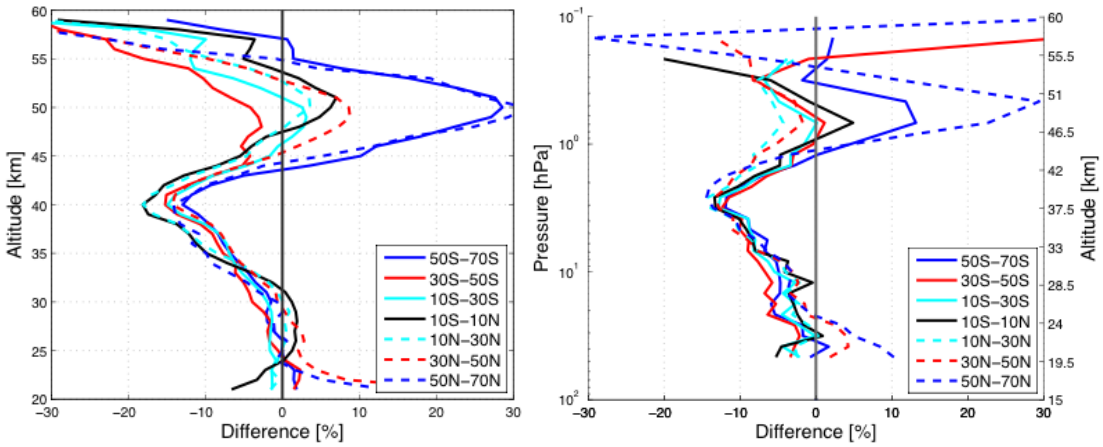

Figure 23: Comparison of the GBL ozone profiles against GOMOS night occultations (left panel) and MLS (right panel). Shown are medians of individual relative differences from 2002-2012 (against GOMOS) and 2004-2012 (against MLS) for several different latitude bands.

5.3. Action plans to develop matured products

We have worked a lot to understand the 40 km bias. This is the region where we switch from UV wavelengths to visible wavelengths in the retrieval. It seems that the GOMOS UV radiances are contaminated by stray light in the 300-320 nm band below 45 km. This stray light is (at least) a function of altitude and solar zenith angle. It is one very likely reason for the bias. In future we could try to further understand the behaviour of this stray light and better deal with it in the retrieval. Also the reason for the high latitude bias in the 50 km tangent altitude is currently unknown. This should be studied in the future.

6. WP 18: Temperature climatologies and comparison to RO

6.1. Status of the products

Temperature climatologies in the form of monthly mean zonal mean time series have been produced from ACE-FTS, MIPAS and SMR, and from radio occultation instruments, including CHAMP, GRACE and TSX. Production of a climatology from GOMOS has been delayed, see below. A radio occultation climatology from COSMIC was also planned to be produced, however, the raw data set is very large and the download has still not been completed. It is estimated that the COSMIC climatology could be available by June 2013.

6.1.1. ACE-FTS

The climatology is based on profiles from retrieval version 3.0. The profile data and climatology are provided by UT (A. Jones / K. Walker).

6.1.2. GOMOS

Profiles from retrieval version HRTP v5 are available but the planned climatology for SPIN should be based on the new v6 retrieval, which is still awaiting validation and data screening before a climatology can be produced. There is no estimated time of delivery. The profile data are provided by ESA and the climatology will be created by FMI (V. Sofieva).

6.1.3. MIPAS

The climatology is based on profiles from the high spectral resolution data (version V3O_T_8) from July 2002 – March 2004 and the reduced spectral resolution data (version V5R_T_220) from January 2005 – April 2010. These data were provided by IMK in cooperation with IAA. The climatology has been produced by IMK/IAA (T. von Clarmann/B. Funke).

6.1.4. SMR

Two climatologies have been produced, based on profile data from the 544.6 GHz band (version 2.0) and the 556.9 GHz band (version 2.1) retrievals, respectively. The profile data and climatology are provided by CUT (J. Urban).

6.2. Data quality

The data quality information presented in this subsection refers to the underlying profile data.

6.2.1. ACE-FTS

The accuracy of the data is estimated to be 2 K at 10-50 km and 5 K at 50-70 km (Sica et al, 2008). No information on the precision is available. The vertical resolution of the ACE-FTS measurements is ~3-4 km resulting from the field-of-view of the instrument (Boone et al, 2005). This information is for the previously validated version (v2.2) and is expected to be similar for v3.0.

6.2.2. GOMOS

The precision of the HRTP v6 data is estimated to be 1-2 K at 18-32 km for best individual profiles. The vertical resolution is ~200 m (Sofieva et al., 2009). In general, precision depends on obliquity of occultations and, to a lesser extent, on stellar brightness. A preliminary validation of the HRTP v6 data presented at the last quality working group meeting of the

VALID-2 (satellite validation with lidar) team has shown agreement of HRTP with radiosonde and lidar data to within a few Kelvin over most altitudes. In comparisons with radiosondes, the difference from zero is not statistically significant. In comparisons with lidar, HRTP seems to be too cold (~3 K) at the top of profiles.

6.2.3. MIPAS

The precision of the high spectral resolution data is 0.4-0.8 K at ~3 km vertical resolution for stratospheric altitudes (von Clarmann et al., 2003). The precision of the reduced spectral resolution data is 0.5-1.4 K at 2-3.5 km vertical resolution at 10-50 km (von Clarmann et al., 2009; Stiller et al., 2012). Bias-corrected root mean squares for the reduced spectral resolution data differences are typically between 2 and 3 K with a pronounced maximum around 17 km reaching values of up to 5 K (Stiller et al., 2012), the latter attributed to less than perfect spatial and temporal co-incidences with the validation instruments in combination with a very instable atmospheric situation leading to large natural variability. For the high spectral resolution data the bias-corrected root mean square differences are 2.5-3.5 K (Wang et al., 2005).

6.2.4. SMR

The precision of the temperature data from the 544.6 GHz and 557 GHz bands is estimated to be 1-3 K, as derived from SMR retrieval diagnostics (error covariance matrices) (Jo Urban, personal communication). Lossow et al. (2007) reported earlier a precision better than 5 K for the 557GHz band, but their work focused mainly on the water vapour retrieval from the same band. No information on the accuracy is available. The vertical resolution for the 544.6 GHz and the 556.9 GHz band is 4-6 km and 5-6 km, respectively (Jo Urban, personal communication).